Genetic and pathogenetic diversity of fowl glioma-inducing viruses

(鶏のグリオーマ誘発ウイルスの遺伝子および病原性の多様性)

Sayuri NAKAMURA

Contents

General introduction

Fowl glioma is histopathologically characterized by multiple nodular astrocytic growths with disseminated non-suppurative encephalitis (Summers *et al*., 1995; Swayne *et al*., 2008). This disease has been described as glioma (Belmonte, 1935; Jackson, 1954), astrocytoma (Jungherr & Wolf, 1939; Reece, 2008), astroblastoma, multiple glioblastoma, mixed gliomatoses (Biering-Sørensen, 1956), epizootic gliosis and astrocytoma (Wight & Duff, 1964). The disease is caused by fowl glioma-inducing virus (FGV) prototype, belonging to subgroup A of avian leukosis virus (ALV-A) (Ochiai, *et al*., 1999; Iwata, *et al*., 2002; Tomioka, *et al.*, 2003). This strain could also induce cerebellar hypoplasia and multiple perineurioma as well as glioma (Toyoda *et al*., 2005; 2006; Ochi *et al*., 2012b).

Avian leukosis/sarcoma viruses (ALSVs), including ALVs, belong to family *Retroviridae*, genus *Alpharetrovirus*. ALVs are virologically and serologically classified into exogenous viruses (subgroup A, B, C, D and J) and endogenous viruses (subgroup E, F, G, H and I), and infection of subgroup A, B and J are most common in chickens (Fadly & Nair, 2008). Although ALVs-A generally induce haematopoietic neoplasms such as lymphoid leukosis (LL) (Fadly & Nair, 2008), FGV prototype show pathogenicity to the nervous system. However, how only a few strains of ALVs show neuropathogenicity remains unclear.

FGV prototype has the specific base sequence in 3’ untranslated terminal region (3’UTR) and nested PCR for this specific region has been used for screening FGV infection (Hatai *et al*., 2005). Epidemiological studies revealed that FGV variants have been prevalent among ornamental Japanese chickens in Japan and the *env* gene of the

isolates frequently had mutations and deletions of nucleotides (Hatai *et al*., 2008a; Ochi *et al*., 2012a). Recently, it has been reported that four strains of ALVs-A isolated from glioma-affected chickens, Km_5666, Km_5843, Km_5844 and Km_5845, did not have the FGV-specific region in their genome. In addition to these strains, TymS_90, which has been isolated from a layer chicken in a flock concurrently affected with fowl glioma and cephalocervical subcutaneous neoplasms (myxoma, fibroma and fibrosarcoma), also lacks the FGV-specific region in the genome. These findings suggest that neuropathogenic ALVs have genetic diversity (Hatai *et al*., 2008b; Ochi *et al*., 2012a).

Furthermore, unusual cardiac abnormality has been found in Japanese native fowls infected with ALVs during epidemiological studies of fowl glioma. The cardiac lesions were characterized by hypertrophied cardiomyocytes with large atypical nuclei and mitosis. Whereas ALVs show broad tissue tropism through systemic organs, ALVs can replicate most excessively in heart compared to other organs (Arshad *et al*., 1999; Tomioka *et al*., 2003). These findings imply that ALVs cause cardiomyopathy and/or myocarditis. The causal relationship, however, is not completely established and pathogenesis of ALV-induced cardiac abnormality remains unclear.

From these backgrounds, serial studies to clarify the pathogenesis of ALV-induced glioma and cardiac abnormality were performed. In Chapter I, in order to elucidate the contribution of the *env* gene to neuropathogenicity of FGVs, FGV variants with mutations of the *env* genes and a chimeric virus, which are the avian retroviral vector RCAS (A) with the SU region of the *env* gene of FGV prototype, were used for experimental infection to chickens and their neuropathogenicity was compared based on the histopathology. In Chapter II, the relationship between intracerebral viral replication and astrocytic growth was analysed using an FGV variant showing most severe brain

lesion in Chapter I. In Chapter III, the morphological features of congenital cerebellar dysplasia in specific-pathogen-free (SPF) chickens were analysed and the difference between it and the cerebellar hypoplasia associated with FGV infection was discussed. In Chapter IV, unusual hypertrophy and mitosis of cardiomyocytes, the morphology of which has not been previously reported in chickens infected with ALVs-A, were described. Additionally, the pathogenesis is discussed on the basis of the molecular characteristics of isolates and the results of a reproducibility experiment with isolates.

Chapter I

Pathogenicity of avian leukosis viruses related to fowl glioma-inducing virus prototype

Introduction

FGV prototype causes the so-called fowl glioma and cerebellar hypoplasia in chickens as previously mentioned. Both the long terminal repeat (LTR) and the *env* genes of ALV are known to play important roles in the oncogenicity and tissue tropism of ALV (Fadly & Nair, 2008). When the provirus is eventually inserted upstream of cellular oncogenes, the LTR domain activates transcription of these genes, resulting in tumour formation (promoter insertion). The envelope glycoprotein of ALV acted as a ligand in binding to the receptors of host cells (Weiss, 1993) and served as a determinant of the tissue tropism of ALV (Brown & Robinson, 1988). As a typical example, the subgroup J of ALV causing myeloid leukosis had the distinct *env* gene from other ALV subgroups that usually produce lymphoid leukosis (Payne, 1998; Arshad *et al*., 1999). Chesters *et al* (2002) constructed chimeric viruses using ALV-A and ALV-J, and revealed that ALV-J with the *env* gene of ALV-A induces lymphoid leukosis whereas ALV-A with the *env* gene of ALV-J induces myeloid leukosis. However, whether FGV variants with mutations and deletions of nucleotides of the *env* gene have neurotropism and/or gliomagenicity remains unclear. In this chapter, the entire viral genome of four FGV variants was analysed and experimental *in ovo* infection was performed to clarify whether or not these strains have the ability to induce central nervous system (CNS) lesions. In addition, the pathogenicity of a chimeric virus constructed by substituting the surface (SU, glycoprotein 85) region of the *env* gene of FGV prototype into the avian retroviral vector RCAS (A) was examined.

Materials and Methods

Virus and cell culture

Twenty-two strains related to FGV prototype were previously isolated from ornamental Japanese chickens kept in zoological gardens in Japan and the phylogenetic results of the 3' untranslated region and the *env* gene of these strains have been described (Hatai *et al*., 2008a). These viruses were detected with nested PCR specific for FGVs (Hatai *et al*., 2005). Among these isolates, four ALV strains, Tym-43, U-1, Sp-40 and Sp-53, were selected from the different phylogenetic groups based on the *env* gene and used in this study.

DF-1 cells were obtained from the American Type Culture Collection (VA, USA). Cell culture was performed according to manufacturer's instruction and preparation of the viral suspension was performed using methods described by Iwata *et al*. (2002). For inoculation, 100-fold concentrated culture supernatant was prepared according to the method described previously (Bowles *et al*., 1996).

A chimeric virus RCAS (A)-(FGV*env*SU) was constructed by substituting the SU region of the *env* gene of FGV provirus (sequence position: 5228-6617, GenBank accession no. AB112690) into the replication-competent ALV-based vector RCAS (A) (kindly donated by Dr. Stephen H. Hughes, National Cancer Institute, USA) (Hughes *et al*., 1987: Hughes, 2004), according to the method described previously (Chesters *et al*., 2002). Described briefly as follows, the SU region of FGV prototype was removed from the full-length FGV prototype genome by digestion with *Kpn*I and *Bfr*I. The RCAS (A) vector, which contains a conserved *Kpn*I restriction site between *pol* and *env* (Bai *et al*., 1995; Bieth & Darlix, 1992), was also digested with *Kpn*I and *Bfr*I (sequence position:

5365–6739). The agarose gel-purified *Kpn*I–*Bfr*I fragment of FGV prototype was ligated to the *Kpn*I–*Brf*I-cut RCAS (A) clone using Mighty mix (TaKaRa Bio, Tokyo, Japan). The complete sequences of the *env* gene of the chimeric plasmid clone and the ligation junctions were determined to rule out any errors introduced during PCR and cloning. The propagation of RCAS (A)-(FGV*env*SU) was initiated by transfection of 1–2 μg of the plasmid DNA into DF-1 cells using FuGENE6 (Roche Diagnostics Ltd., Mannheim, Germany).

RNA extraction and cDNA synthesis

Total RNA was extracted from cultured DF-1 cells using TRIzol reagent (Life Technologies, CA, USA). Reverse transcription (RT) was performed as previously described (Hatai *et al.*, 2008b). As an internal control for RNA extraction and cDNA synthesis, PCR amplification was performed for all cDNA samples using primers specific to chicken β-actin (Table 1). The PCR products were analysed by 2% agarose gel electrophoresis.

Sequencing analysis

The entire viral genome was sequenced using the cDNA sample of each isolate as previously described (Tomioka *et al*., 2004; Hatai *et al.*, 2008b). PCR amplification was performed with three primer pairs, LTRfwd and Prev, GrevF and AD1, or H5 and IP-LTRrev (Table 1), using GeneAmp PCR System 9700 (Life Technologies) in Max ramp speed mode. Sequencing was conducted by Bio Matrix Research (Chiba, Japan). Computational sequence analysis was done using CLUSTAL W 1.8.3 (Thompson *et al*., 1994) combined with a search of GenBank using the NCBI BLAST program to

Table 1. Sequences of oligonucleotide primers and targets.

Primer	Sequence (5' - 3')	Primer position	Accession number
chicken β-actin fwd	TAT CCG TAA GGA TCT GTA TG	932 to 951	L08165
chicken β-actin rev	ATC TCG TCT TGT TTT ATG CG	1250 to 1269	L08165
LTRfwd	ACC ACA TTG GTG TGC ACC TGG GT	16 to 38	AB112960
Prev	TGC AAT AAG CGA TAA GAC CC	2720 to 2701	AB112960
GrevF	CTT AGT TGT TGG AAC ACG CCT GTC	2656 to 2679	AB112960
AD1	GGG AGG TGG CTG ACT GTG T	5327 to 5345	V01197
H5	GGA TGA GGT GAC TAA GAA AG	5258 to 5277	Z46390
IP-LTRrev	CCA GGT GCA CAC ACC AAT GTG GTGG G	7451 to 7463	AB112960
ALV#38	TTA GGT TCC CAG TCT CTC CC	5570 to 5589	AB112960
ALV#39	ATT GCG GGT GGT AGC GCT TT	6126 to 6107	AB112960
Real Time ev1F	TGG AAA GGT GAG CAA GAA GGA	5101 to 5121	AB112960
Real Time ev1R	CAC ACA AGACCA GGA CAC CAA	5208 to 5228	AB112960
RealTime BactinF2	TGG CAC CTA GCA CAA TGA AAA	1027 to 1047	L08165
RealTime BactinR	GAC AGG GAG GCC AGG ATA GA	1098 to 1117	L08165

check the homology with known ALSV gene sequences. In experimental infection, total RNA was extracted from the cerebrum of each isolate-inoculated chicken. PCR amplification was performed using the primer set ALV#38 and ALV#39 as described previously for sequencing the hypervariable region in the SU region of the *env* gene (Table 1; Ono *et al.*, 2004). Other procedures for sequencing were the same as described above.

Semi-quantitative real-time RT-PCR of viral RNA

Quantitative real-time RT-PCR was performed using a 7300 Real-Time PCR System (Life Technologies) with SYBR-Green as a double-stranded DNA Specific fluorescent dye. Primer pairs were RealTime ev1F and RealTime ev1R, and RealTime BactinF2 and RealTime BactinR (Table 1). Amplification mixes were 20 μl reaction volume containing 2 μl cDNA, 10 μl SYBR premix Ex TaqII (TaKaRa Bio), 0.8 μl each primer (10 μM), 0.4 μl ROX Reference Dye (50x), and 6 μl water. The detector system was programmed to start with an activation step for 1 min at 95°C followed by a PCR program with 40 cycles of 10 sec at 95°C and 30 sec at 60°C. The standard curve was plotted based on the results of 10x, 20x, 40x, 80x and 160x diluted cDNA from FGV-infected DF-1. To normalize the data, the cycle threshold (CT) values of the housekeeping gene chicken β-actin were subtracted from the target gene CT value of the sample (= dCT). Statistical differences in the quantitative levels of viral RNA were assessed among examined groups by Student's *t* test. $P < 0.05$ was accepted as the level of statistical significance.

Histopathology and immunohistochemistry

The brains and other organs, including the liver, spleen, kidney, heart and lung were fixed in 20% neutral-buffered formalin, routinely processed, and embedded in paraffin wax. Sections (4 μm) were cut and stained with haematoxylin and eosin. Immunostaining using the labelled streptavidin-biotin method (Nichirei Corp, Tokyo, Japan) was performed for glial fibrillary acidic protein (GFAP) and ALV antigens, using primary antibodies of rabbit anti-cow GFAP (Dako, Copenhagen, Denmark) and anti-ALV antibodies at 1 in 2,500 and 1 in 5,000 dilution, respectively. The polyclonal antibody against ALVs was generated by immunization of rabbits with Rous associated virus-2 as previously described (Tsukamoto *et al*., 1991; K. Tsukamoto, personal communication, 2001). This antibody recognized mainly gp85 and p27 of ALVs.

Animals and experimental infection

Fertile eggs from specific pathogen-free (SPF) chickens of the WL-M/O (C/O) strain were purchased from Nippon Institute for Biological Science (Yamanashi, Japan) and used in the animal infection experiment. This strain lacks both chicken helper factor and group-specific antigen and is susceptible to ALV subgroups A to E (International Registry of Poultry Genetic Stocks, Bulletin 476, March 1988, Ralph G. Somes, Jr., Ph.D., University of Connecticut, USA). The presence of endogenous virus genes other than chicken helper factor and group-specific antigen was unidentified. These chicken embryos were inoculated via the yolk sac on the sixth day of incubation with 0.1 ml viral suspension and were euthanized at 35 and 70 days of age. Seven control chicken embryos were similarly inoculated with 0.1 ml uninfected tissue culture medium and

were euthanized at 35 (n=3) and 70 days (n=4) of age. As a control for the RCAS (A)-(FGV*env*SU)-inoculated group, seven embryos were inoculated with RCAS (A). The hatched chickens were reared in isolators in the animal facilities of our institution. All experiments were performed humanely according to the guidelines set by Animal Care and Use Committee of Graduate School of Veterinary Medicine, Hokkaido University (Permission numbers: 8120 and 9013). No chickens received any vaccinations or medication.

Accession number

The nucleotide sequence data of the four isolates (Tym-43, U-1, Sp-40 and Sp-53) appeared in the EMBL, GenBank and DDBJ nucleotide sequence databases under accession numbers AB617817, AB617818, AB617819 and AB617820, respectively.

Results

Analysis of the entire viral genome of four isolates

The entire viral genome sequences of four strains related to FGV prototype, Tym-43, U-1, Sp-40 and Sp-53 showed 90 to 96% identity with that of FGV prototype (Table 2). The *gag* and *pol* genes of these isolates showed more than 96% identity with the corresponding regions of FGV prototype, indicating that these genes were well conserved among those of FGVs. In the SU coding sequences of the *env* genes, the identities of Tym-43, U-1, Sp-40 and Sp-53 with the corresponding region of FGV prototype were 95%, 95%, 85% and 85%, respectively. Sp-40 and Sp-53 showed the

Table 2. Sequence homology of four isolates with the corresponding regions of FGV prototype (%).

				env			
	entire viral genome	*gag*	*pol*	whole	SU	TM	3' LTR
Tym-43	96	97	97	94	95	93	93
U-1	96	96	98	94	95	94	93
Sp-40	90	96	97	89	85	93	93
Sp-53	90	96	97	89	85	93	93

lowest identity, mainly due to deletions and frequent nucleotide substitutions in the hypervariable regions. Phylogenic analysis of the SU regions of the *env* gene revealed that Tym-43, U-1 and FGV prototype were categorized into the same group, while Sp-40 and Sp-53 formed a completely separate cluster (Figure 1). There were a few insertions and deletions in the 3' LTR (U3/R elements) of these strains and FGV prototype compared with the corresponding regions of ALV-RSA, a standard strain of ALV-A. However, the 3' LTR of each isolate showed 93% identity with FGV prototype, and all isolates and FGV prototype were grouped into the same cluster on the phylogenetic tree based on the nucleotide sequences in this region.

Clinical signs and pathology

One of three (33%) U-1-inoculated chickens at 70 days of age showed mild elevation of the left leg. Other chickens inoculated with each isolate, RCAS (A)-(FGV*env*SU), RCAS (A) and medium showed no clinical sign. Grossly, the cerebellum from one of three (33%) birds at 35 days of age and two of four (50%) birds at 70 days of age in the Sp-53-inoculated group had irregularly-shaped foliar disorganization of cerebellar vermis (Figure 2a). Similar lesions were noted in the cerebellum of one of six (17%) birds at 35 days of age and one of three (33%) birds at 70 days of age in the U-1-inoculated group. No gross lesion was seen in any organs of the other chickens.

Histologically, all chickens inoculated with each isolate, including 17 chickens at 35 days of age and 14 birds at 70 days of age, had varying degrees of non-suppurative encephalitis in the brain (Table 3). Severe perivascular cuffing in the cerebrum and cerebellum was observed in one of nine (11%) U-1-inoculated chickens and in two of

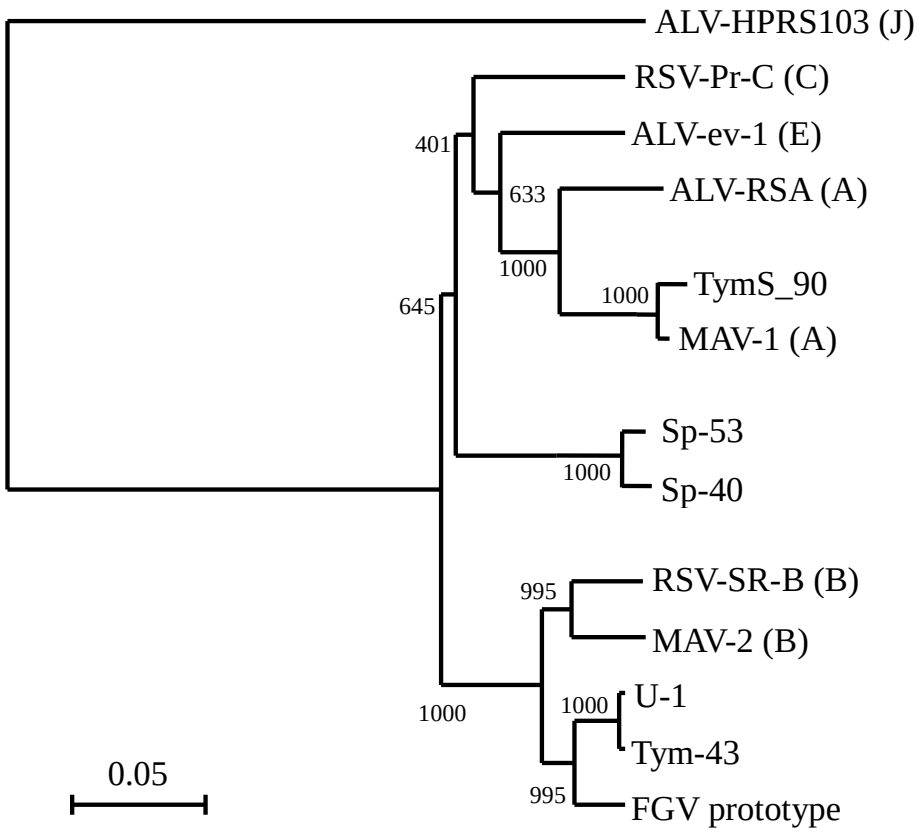

Figure 1. Phylogenic tree constructed based on the SU region of the *env* gene (neighbour-joining method). This tree shows the relationships between the strains related to FGV prototype and ALSVs based on the SU region of the *env* gene. Numbers at bifurcations indicate the bootstrap values. The name of standard ALSVs and/or GenBank accession numbers are as follows: RSV-SR-B, Rous sarcoma virus Schmidt-Ruppin B (AF052428); RSV-Pr-C, Rous sarcoma virus Prague C (J02342); MAV-1, myeloblastosis-associated virus type 1 (L10922); MAV-2, myeloblastosis-associated virus type 2 (L10924); ALV-RSA (M37980); ALV-*ev*-1 (AY13303); ALV-HPRS103 (Z46390); Letters in parentheses show the subgroup of each ALSV.

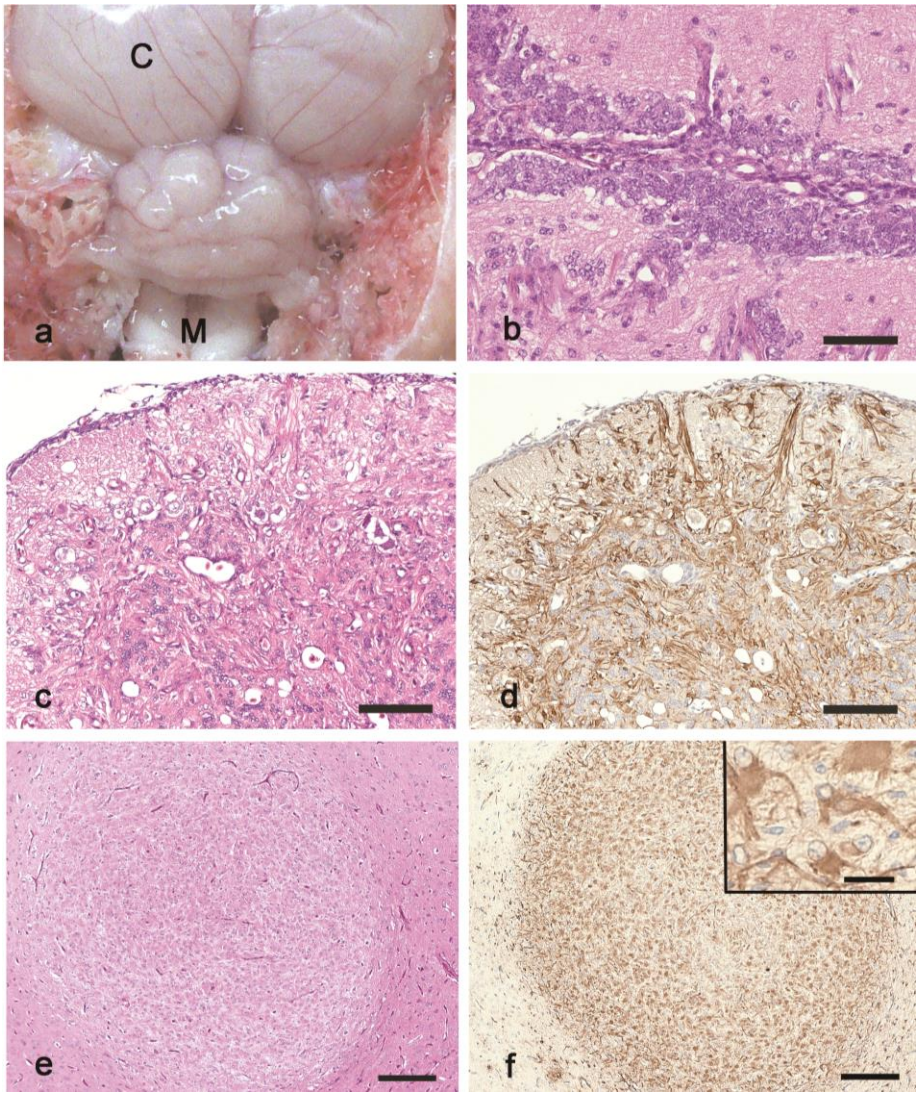

Figure 2. Gross lesion, histopathology and immunohistochemistry of chickens inoculated *in ovo* with four strains related to FGV prototype at 70 days of age. a: Irregularly shaped foliar disorganization of cerebellar vermis in an Sp-53-inocualted chicken. C, left cerebral hemisphere; M, medulla oblongata. b: Severe remnant of external granular layer and aggregation of granular cells with proliferation of blood vessels in the molecular layer of cerebellum of an Sp-53-inoculated chicken. Haematoxylin and eosin (HE) stain. Bar = 50 μm. c: Diffuse absence of granular cells of the internal granular layer and disorganization of the Purkinje cell layer in cerebellar cortex. Sp-53-inoculated chicken. HE stain. Bar = 100 μm. d: GFAP-positive astrocytes diffusely proliferate (gliosis) in the same region as Figure 2c. Streptavidin-biotin complex, haematoxylin. Bar = 100 μm. e: Nodular proliferation of astrocytes in cerebrum of an Sp-40-inocualted chicken. HE stain. Bar = 200 μm. f: Fowl glioma consisting of GFAP-positive astrocytes in the same area as Figure 2e. Streptavidin-biotin complex, haematoxylin. Bar = 200 μm. Inset: higher magnification of intranodular astrocytes. Bar = 20 μm.

Table 3. Frequency and degree of brain lesions in chickens inoculated with four isolates related to FGV prototype, RCAS (A)-(FGVenvSU) and RCAS (A).

			Perivascular cuffing				Remnant of external granular layer in cerebellum				Disorganization of Purkinje cell layer in cerebellum				Gliosis[a]				Glioma[b]			
Inoculum (*in ovo*)	Age (days)	N	-	+	++	+++	-	+	++	+++	-	+	++	+++	-	+	++	+++	-	+	++	+++
Tym-43	35	5	0	4	1	0	0	4	1	0	4	0	1	0	4	1	0	0	3	2	0	0
	70	4	0	4	0	0	0	3	1	0	3	1	0	0	0	4	0	0	3	1	0	0
U-1	35	6	0	2	3	1	0	1	5	0	4	1	0	1	5	1	0	0	5	1	0	0
	70	3	0	2	1	0	0	1	2	0	0	1	1	1	1	2	0	0	1	2	0	0
Sp-40	35	3	0	2	1	0	0	1	2	0	2	0	1	0	2	0	1	0	1	1	0	1
	70	3	0	1	2	0	0	2	1	0	1	1	1	0	0	1	0	2	1	0	0	2
Sp-53	35	3	0	0	3	0	0	0	2	1	0	0	1	2	0	1	1	1	0	0	2	1
	70	4	0	0	2	2	0	1	1	2	0	0	1	3	0	0	1	3	0	0	2	2
RCAS (A)-	35	3	3	0	0	0	3	0	0	0	3	0	0	0	3	0	0	0	3	0	0	0
(FGVenvSU)	70	4	2	2	0	0	4	0	0	0	4	0	0	0	4	0	0	0	4	0	0	0
RCAS (A)	35	3	3	0	0	0	3	0	0	0	3	0	0	0	3	0	0	0	3	0	0	0
	70	4	3	1	0	0	4	0	0	0	4	0	0	0	4	0	0	0	4	0	0	0

[a] Clusters consisting of less than 10 astrocytes were considered as gliosis

[b] A solid growth of more than 10 atypical astrocytes that was clearly distinguishable from the surrounding tissue was described as Glioma. The degree of glioma was defined as follows. +: single nodule or multiple nodular growth (under 35 μm in diameter) of astrocytes, ++: multiple nodular growth (from 35 to 55 μm in diameter), +++: multiple nodular growth (over 55 μm in diameter).

seven (29%) Sp-53-inoculated birds. Also, three of seven (43%) Sp-53-inoculated chickens showed a severe remnant of the external granular layer in the cerebellum (Figure 2b), while the degree of the lesion was mild to moderate in chickens inoculated with the other three isolates. Cerebellar hypoplasia, which was characterized by disorganization of the Purkinje cell layer, was found in all of seven (100%) Sp-53-inocualted birds (Figure 2c), five of nine (56%) U-1-inoculated birds, three of six (50%) Sp-40-inocualted birds and two of nine (22%) Tym-43-inoculated birds. In the cerebellum, granular cells frequently aggregated with vascular proliferation in the molecular layer and astrocytes multifocally to diffusely proliferated in the cerebellar cortex and medulla (Figure 2d). Clusters consisting of less than 10 astrocytes were indistinguishable from gliosis, whereas the gliomas consisted of the solid growth of more than 10 atypical astrocytes and were clearly distinguishable from the surrounding tissue. Seventeen of 31 (55%) chickens inoculated with either isolate had multiple gliomas and 19 (61%) showed gliosis. Moderate to severe glioma were found in all Sp-53-inoculated chickens and in three of six (50%) Sp-40-inoculated birds, and most proliferating astrocytes were positive for ALV antigens and GFAP (Figure 2e and 2f). Two of seven (29%) RCAS (A) - (FGV*env*SU)-inoculated chickens and one of seven (14%) RCAS (A)-inoculated birds had only mild perivascular lymphocytic infiltration in the brain. No microscopic lesion was observed in the control brains inoculated with medium.

Recovery of viral RNA in experimental infection

RNA extracts were obtained from the cerebrum of a 35-day-old chicken and a 70-day-old chicken in each inoculated group and sequence analysis of the variable

regions in the SU of the *env* gene was performed to confirm the identity between the inocula and the recovered viruses after the experimental infections. The sequence identity between them in each group ranged from 99.4 to 100 %. In addition, viral RNA in the cerebrum of 70-day-old chickens (n = 3 or 4) in each group was semi-quantified with real-time PCR. Viral RNA was detected in all virus-inoculated groups, but the Tym-43-inoculated, Sp-40-inoculated and Sp-53-inoculated groups showed a significantly lower level of viral RNA than RCAS (A)-(FGV*env*SU)-inoculated and RCAS (A)-inoculated groups (Figure 3). There was no significant difference between any of the four isolate-inoculated groups. The PCR products were not detectable in the cerebrum of the control chickens.

Discussion

The present study demonstrated that the four isolates were variants of the FGV prototype and they could induce fowl glioma and cerebellar hypoplasia. In contrast, no CNS lesion related to fowl glioma was seen in the chickens inoculated with the retroviral vector RCAS (A) and the chimeric virus RCAS (A)-(FGV*env*SU).

Phylogenic analysis revealed that Tym-43 and U-1 were more closely related to FGV prototype than Sp-40 and Sp-53. In the experimental infection, CNS lesions were most frequently and severely observed in Sp-53-inoculated chickens. Furthermore, Sp-40 belonging to the same cluster as Sp-53 based on the SU region of the *env* gene also induced severe glioma. In previous reports (Tomioka *et al*., 2003; Toyoda *et al*., 2006), the frequency of fowl glioma in chickens experimentally infected with FGV

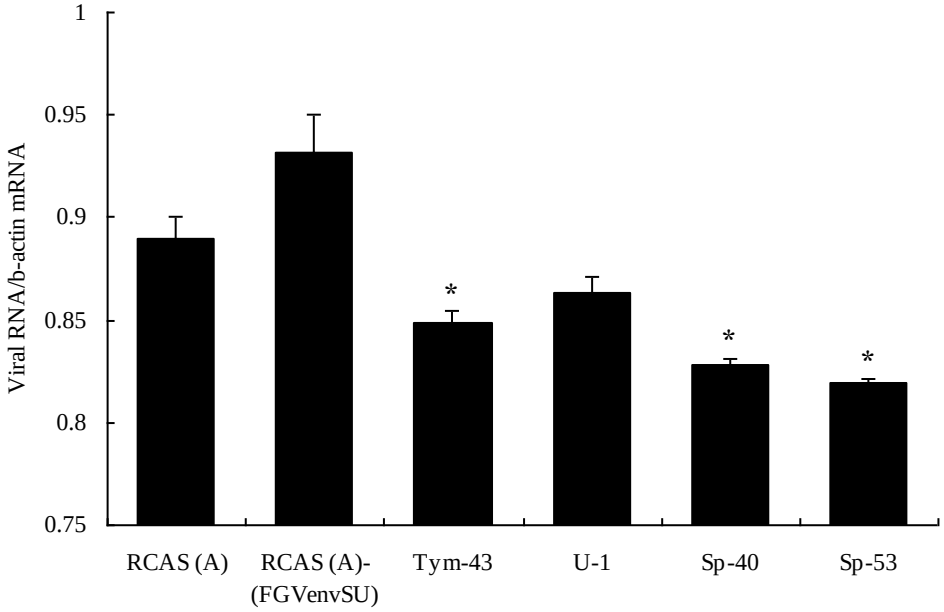

Figure 3. Levels of viral RNA in cerebrum of chickens at 70 days of age with the real-time PCR. Histograms represent the means ± standard errors of the means (n = 3 or 4) of viral RNA levels expressed as a ratio to that of the β-actin mRNA level (* $p<0.05$).

prototype was less than 14% at 50 to 70 days of age and the inoculated birds showed no grossly visible cerebellar hypoplasia except for a mild decrease in size. The results in this study suggest that these variants could be useful materials for further investigations using recombinant chimeric viruses to elucidate the neuropathogenicity of fowl glioma-inducing ALVs. In the current study, however, it could not be concluded that whether the differences in severity and frequency of CNS lesions were due to viral load and/or due to genetic differences because virus dosage of each experimental group has not been strictly conformed.

On the other hand, RCAS (A) and RCAS (A)-(FGV*env*SU) induced only mild non-suppurative encephalitis. Because one strain of ALVs-A, Rous associated virus-1 (RAV-1), experimentally induced non-suppurative encephalitis (Ewert *et al*., 1990), several strains of ALVs-A may have the ability to induce non-suppurative encephalitis in chickens. These results show that the *env* gene appears to be a minor determinant to cause fowl glioma.

Two mechanisms of pathogenesis are conceivable to explain the pathologic changes in the so-called fowl glioma: 1) direct effects and host responses by viral infection and 2) activation of an oncogene after ALV proviral integration. Lymphocytic infiltration in the CNS is considered to be an inflammatory response to viral infection, and cerebellar hypoplasia associated with FGV prototype is suggested to be due to the apoptosis of granular cells in the external granular layer and molecular layer caused by viral infection (Toyoda *et al*., 2006). Whether nodular gliomatous proliferation is a true neoplasm is still controversial, as described by Luginbühl *et al.* (1968), because the specific viral oncogene is not determined and the occurrence time of gliomatous foci is too short compared to that of lymphoid leukosis, which is induced in chickens of about

4-5 months of age and older by slowly transforming viruses (Fadly & Nair, 2008). The possibility that nodular lesions are directly related to the rapid and abundant replication of FGVs in the brains cannot be ruled out.

In conclusion, the present study shows that FGV variants with 85 to 95% identity of the SU region of the *env* gene of the FGV prototype still could have the ability to induce CNS lesions.

Summary

FGV prototype, which belongs to ALV-A, causes the so-called fowl glioma and cerebellar hypoplasia in chickens. In this chapter, the complete nucleotide sequences of four isolates (Tym-43, U-1, Sp-40 and Sp-53) related to the FGV prototype were determined and their pathogenicity was investigated. Phylogenic analysis showed that the 3'-long terminal repeat of all isolates grouped together in a cluster, while sequences of the surface (SU) proteins encoded by the *env* gene of these viruses had 85 to 95% identity with the corresponding region of FGV prototype. The SU regions of Tym-43, U-1 and FGV prototype grouped together in a cluster, but those of Sp-40 and Sp-53 formed a completely separate cluster. Next, C/O specific-pathogen-free chickens were inoculated *in ovo* with these isolates as well as the chimeric virus RCAS (A)-(FGV*env*SU), constructed by substituting the SU region of FGV prototype into the retroviral vector RCAS (A). The four variants induced fowl glioma and cerebellar hypoplasia and the birds inoculated with Sp-53 have the most severe lesions. In contrast, RCAS (A)-(FGV*env*SU) provoked only mild non-suppurative inflammation. These results suggest that the ability to induce brain lesions similar to those of the FGV prototype is still preserved in these FGV variants and the SU region of the *env* gene is not a crucial determinant to glioma-inducibility of FGVs.

Chapter II

Astrocytic growth through the autocrine/paracrine production of IL-1β in the early infection phase of fowl glioma-inducing viruses

Introduction

The main brain lesions of so-called fowl glioma could be histologically divided into three types, non-suppurative inflammation, gliosis and glioma (Iwata *et al*., 2002). Perivascular cuffing, microgliosis and subependymal gliosis are scattered throughout brains at initial infection phase. After then, astrocytes proliferate in response to these inflammatory reactions and some of astrocytes seem to develop discrete neoplastic nodules (fowl glioma). FGV prototype has a unique sequence in the 3'UTR domain and this sequence is not detected in standard strains of ALVs (Tomioka *et al*., 2004). Fifty-seven FGV variants have been isolated from cloaca swab or brain tissue of Japanese chickens in culture and these isolates were confirmed to have the FGV-specific region in their genome by FGV-specific nested PCR (Hatai *et al*., 2005: Ochi *et al*., 2012a). The phylogenic analysis of the *env*SU region of these variants indicated that these FGVs evolved dividing into three clusters. In addition, studies in Chapter I revealed that FGV variants with 85-95% identity of *env*SU compared with corresponding region of FGV prototype still have the ability to induce brain lesions but the frequency and severity of astrocytic proliferation is different among them. However, the possibility that nodular lesions of astrocytes are directly related to the rapid and abundant replication of FGVs in the brains could not be ruled out in the study of Chapter I.

Although other retroviruses, including human immunodeficiency virus type 1 (HIV-1), human T lymphotropic leukemia virus (HTLV) and simian immunodeficiency virus (SIV), occasionally cause non-suppurative encephalitis, only limited strains of ALVs-A can induce marked astrocytic growth. Cytokine expression has important roles

in various diseases, including infection diseases, neoplasms and autoimmune diseases. Among various cytokines, a proinflammatory cytokine, IL-1β, plays key roles in infection diseases and tumours. Up-regulation of IL-1β has been reported in brains infected with HIV-1 (Merrill & Chen, 1991), highly pathogenic avian influenza virus (Wang *et al*., 2008) and Marek's disease virus (MDV) (Parvizi *et al*., 2010). IL-1β is also up-regulated in primary cultured astrocytes from HIV-1-infected patients, which suggests that this cytokine is an important factor for the neuropathogenesis of HIV-1 (Coyle-Rink *et al*., 2002). On the other hand, the proliferation and survival of astrocytes could be promoted by IL-1β in the microenvironment of human glioblastoma (Sen, 2011; Sharma *et al*., 2011; Yeung *et al*., 2013).

Therefore, intracerebral viral load and the amount of cytokines in the early infection phase of a FGV variant was investigated to clarify whether they are associated with astrocytic growth of fowl glioma in this chapter.

Materials and methods

Virus and cell culture

Sp-53 is one of the strains that were isolated from a Japanese chicken affected with fowl glioma; it induced the most severe brain lesions in Chapter I. A replication-competent ALV-based vector, RCAS (A), was kindly donated by Dr. Stephen H. Hughes.

DF-1 cells were obtained from the American Type Culture Collection. Cell culture and preparation of the viral suspension were performed using methods described in

Chapter I. The propagation of RCAS (A) was initiated by transfection of 1 μg of plasmid DNA into DF-1 cells using FuGENE HD transfection reagent (Promega, WI, USA), according to the manufacturer's instructions. For inoculation, 100-fold concentrated culture supernatant was prepared according to the method described by Bowles *et al*. (1996).

Primary chicken astrocytic culture was prepared by a method described previously (Peters *et al*., 2005). DF-1 cells and primary chicken astrocytes were infected with Sp-53 and RCAS (A) by adding viral suspension containing $5x10^4$ tissue culture infectious unit (TCIU) of each virus. After infection, cell supernatants were collected every 24 hours and cultured cells were collected at intervals of 3 days until 9 days post-infection.

Birds and experimental infection

Fertile eggs of the commercial SPF White Leghorn strain WL-M/O were purchased from Nippon Institute for Biological Science and used for experimental infection. Chicken embryos were inoculated via the yolk sac on the sixth day of incubation with $5x10^2$, $5x10^4$ or $5x10^6$ TCIU of Sp-53 or $5x10^6$ TCIU of RCAS (A). These chickens were euthanized at 35 days of age. The hatched chickens were reared humanely according to the guidelines set by the Animal Care and Use Committee of Graduate School of Veterinary Medicine, Hokkaido University (Permission number: 1148). No chickens received any vaccinations or medication.

Histopathology and immunohistochemistry

Histological examination was performed as described in Chapter I. The scores of

histopathologic changes were defined as follows. Grade 0, no lesions; Grade 1, only perivascular cuffing; Grade 2, perivascular cuffing with microglial infiltration; Grade 3, astrocytic growth consisting of fewer than 10 astrocytes in addition to Grade 2 lesion; Grade 4, astrocytic growth consisting of more than 10 astrocytes in addition to Grade 2 lesion; and Grade 5, multiple astrocytic growth with Grade 2 lesion. Immunostaining using the labelled streptavidin-biotin method (Nichirei Corp) was performed for GFAP and IL-1β, using primary antibodies of rabbit-anti-cow GFAP (Dako) at 1:2,500 dilution and rabbit-anti-IL-1β (Biorbyt, Cambridge, UK) at 1:200 dilution.

RNA extraction and cDNA synthesis

Extraction of total RNA from brains, cultured primary chicken astrocytes and DF-1 cells was performed as described in Chapter I. RNA in each sample was quantified using an ND-1000 spectrophotometer (Nanodrop Technologies, Inc., Wilmington, DE, USA). 1,000 ng of RNA from each sample was used to produce cDNA. Reverse transcription (RT) was performed as previously described (Hatai *et al*., 2008b). As an internal control for RNA extraction and cDNA synthesis, PCR amplification was performed for all cDNA samples using primers specific to chicken β-actin. Primer sequences were indicated in Table 1 in Chapter I. The PCR products were analysed by 2% agarose gel electrophoresis.

Quantitative real-time RT-PCR.

Quantitative real-time RT-PCR (qRT-PCR) was performed using primers described in Table 4 and the StepOne Real Time PCR system (Life Techinologies). Amplified mixtures were 20 μl reaction volumes containing 1 μl of cDNA, 10 μl of Fast SYBR

Table 4. Sequence of the oligonucleotide primers used in quantitative RT-PCR.

Target gene		Sequence (5'-3')	Primer position	Accession No.	Reference
β-actin	F	TGG CAC CTA GCA CAA TGA AAA	1027 to 1047	L08165	Chapter I
	R	GAC AGG GAG GCC AGG ATA GA	1098 to 1117		
ALV-A	F	TGG AAA GGT GAG CAA GAA GGA	5101 to 5121	AB112960	Chapter I
	R	CAC ACA AGA CCA GGA CAC CAA	5208 to 5228		
IL-1β	F	GCT CTA CAT GTC GTG TGT GAT GAG	1030 to 1053	AJ245728	Shini *et al*., 2010
	R	TGT CGA TGT CCC GCA TGA	1179 to 1196		
TGFβ	F	AGG ATC TGC AGT GGA AGT GGA T	862 to 883	M31160	Shini *et al*., 2010
	R	CCC CGG GTT GTG TTG GT	982 to 998		
IL-4	F	AAC ATG CGT CAG CTC CTG AAT	274 to 294	AJ621249	Shini *et al*., 2010
	R	TCT GCT AGG AAC TTC TCC ATT GAA	348 to 371		
IL-6	F	GCT CGC CGG CTT CGA	1020 to 1034	AJ250838	Kaiser *et al*., 2000
	R	GGT AGG TCT GAA AGG CGA ACA G	1186 to 1207		
IFN-α	F	ATG CCA CCT TCT CTC ACG AC	132 to 151	EU367971	Adams *et al*., 2009
	R	AGG CGC TGT AAT CGT TGT CT	499 to 518		
IFN-β	F	CCT CAA CCA GAT CCA GCA TT	333 to 352	AY831397	Adams *et al*., 2009
	R	GGA TGA GGC TGT GAG AGG AG	572 to 591		
IFN-γ	F	GTG AAG AAG GTG AAA GAT ATC ATG GA	4682 to 4707	Y07922	Shini *et al*., 2010
	R	GCT TTG CGC TGG ATT CTC A	5375 to 5393		

Green Master Mix (2x), 0.4 µl of each primer (10 µM) and 8.2 µl of water. PCR conditions were the same for each targeted gene and were as follows: 20 sec at 95 °C followed by 40 cycles of 3 sec at 95 °C and 30 sec at 60 °C.

Enzyme-linked immunosorbent assay

ALV common antigen (p27) in the supernatant of the cell culture was measured using enzyme-linked immunosorbent assay (ELISA), Avian Leukosis Virus Antigen Test Kit (IDEXX Laboratories, Inc., Westbrook, USA), following the manufacturer's instructions.

Calculations and statistics

Expression of each target gene was determined by the -ΔΔCt method using β-actin as an endogenous reference gene to normalise the level of target gene expression. Logarithmic transformation was performed on each value before analysis by Student's *t*-test, ANOVA test and Kruskal-Wallis test. $P<0.05$ was accepted as the level of statistical significance.

Results

Glioma-inducibility in chickens inoculated with different viral loads

Chickens inoculated with three different viral titres of Sp-53 were histopathologically analysed and the mRNA expression of cytokines in brains was evaluated. Multiple astrocytic growth (Figure 4a and 4b) was observed in three (60%)

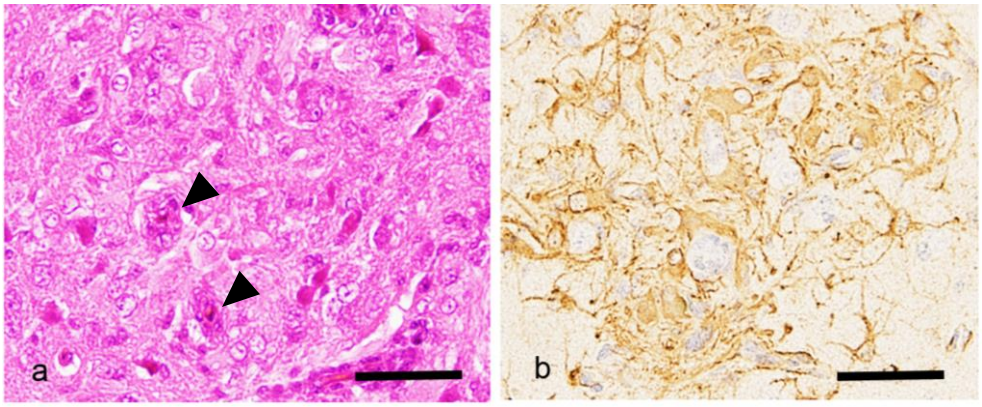

Figure 4. Nodular astrocytic growth in brain of a chicken inoculated *in ovo* with $5x10^4$ TCIU of Sp-53. a: Protoplasmic astrocytes proliferate around vessels (arrowhead). HE stain. Bar = 20 μm. b: Astrocytes in nodules show positivity for GFAP. Immunohistochemistry. Bar = 20 μm.

of five chickens inoculated with $5x10^6$ TCIU and two (67%) of three chickens inoculated with $5x10^4$ TCIU. In contrast, chickens with $5x10^2$ TCIU had no astrocytic growth. Histological scores were significantly higher in $5x10^4$ and $5x10^6$ TCIU-inoculated groups than in the $5x10^2$ TCIU-inoculated group (Figure 5a). Intracerebral viral RNA levels were also greater in $5x10^6$ TCIU-inoculated chickens than in $5x10^2$ TCIU-inoculated ones (Figure 5b). The mRNA levels of IL-1β in the brains were much higher in the $5x10^6$ TCIU-inoculated group than in the $5x10^2$ TCIU-inoculated one, which depended on the viral mRNA levels in the brains. The mRNA levels of TGF-β were increased in the $5x10^4$ TCIU-inoculated group compared to those in the $5x10^2$ TCIU-inoculated group (Figure 5c), although there was no significant difference between $5x10^2$ and $5x10^6$ TCIU-inoculated groups.

Glioma-inducibility of Sp-53

Sp-53 induced multiple astrocytic growth in three (60%) of five inoculated chickens. However, RCAS (A) induced only minimal gliosis, which consisted of fewer than 10 astrocytes in two (40%) of five inoculated animals and showed no gliomatous growth. According to the scoring system described in the Materials and Methods, the Sp-53-inoculated group revealed a significantly higher histological score than the RCAS (A)-inoculated group (Figure 6a). Real-time PCR analysis showed that viral RNA levels were significantly higher in the brains of Sp-53-inoculated chickens than in RCAS (A)-inoculated ones (Figure 6b). The mRNA expression of IL-4 was up-regulated in the brains of RCAS (A)-inoculated chickens compared to that in Sp-53-inoculated ones, whereas the mRNA levels of TGF-β were significantly up-regulated and the RNA levels of IL-1β were considerably higher in the brains of

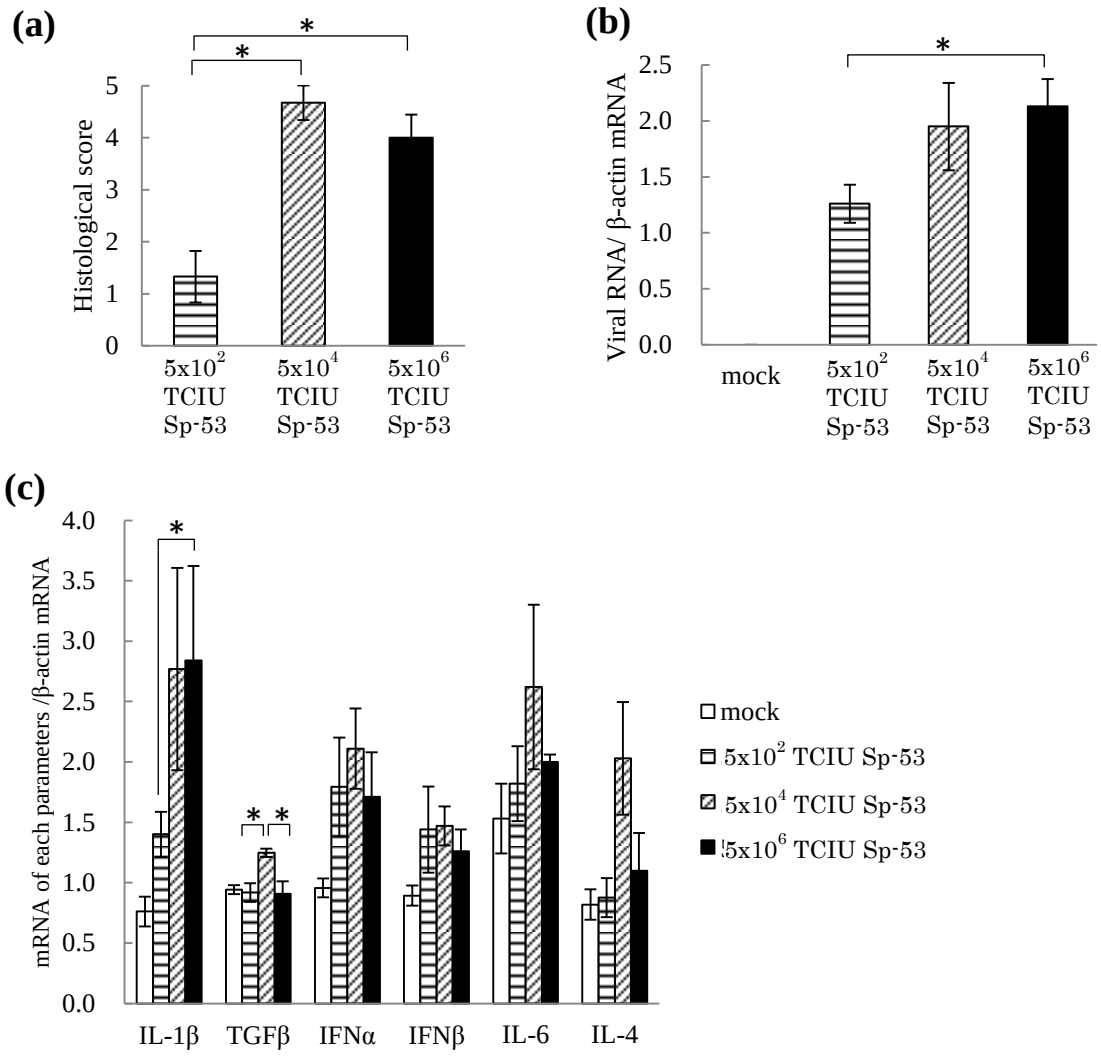

Figure 5. (a) Histopathologic score of chicken brains in each group. The scores of histopathologic changes were defined as described in materials and methods. (b) The level of viral RNA in brains. (c) The expression of cytokines in brains. The level of each cytokine mRNA was calculated by the $-\Delta\Delta Ct$ method. All results were obtained in duplicate. (*) indicates $p<0.05$ for the comparison of each group as determined by ANOVA and Kruskal-Wallis test. Histograms represent the means ± standard errors of the means (n = 3, 6, 3 and 5 in mock, $5x10^2$, $5x10^4$ and $5x10^6$ TCIU Sp-53-inoculated groups, respectively).

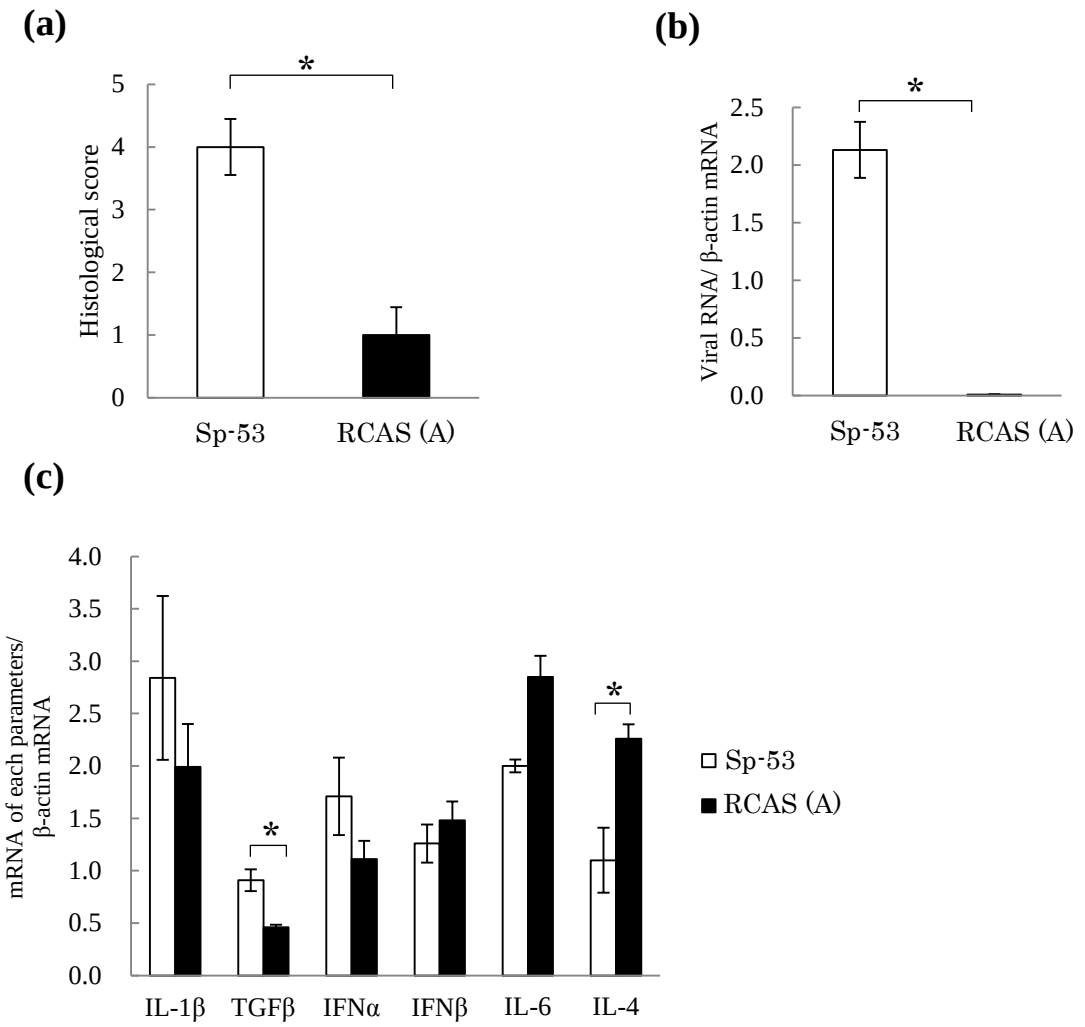

Figure 6. (a) Histopathologic score of chicken brains in each group. The scores of histopathologic changes were defined as described in materials and methods. (b) The level of viral RNA in brains. (c) The expression of cytokines in brains. The level of each cytokine mRNA was calculated by the $-\Delta\Delta Ct$ method. All results were obtained in duplicate. (*) indicates $p<0.05$ for the comparison of two groups as determined by Student's *t*-test. Histograms represent the means ± standard errors of the means (n = 5 in each group).

Sp-53-inoculated chickens than in those of RCAS (A)-inoculated ones (Figure 6c).

Viral replication in DF-1 cells and primary chicken astrocytes

Replication kinetics of Sp-53 and RCAS (A) were estimated in DF-1 fibroblasts and primary cultured astrocytes. ALV common antigen p27 and viral RNA of both viruses were detected from 2 days post-infection (d.p.i.) in DF-1 cells (Figure 7a and 7b) and Sp-53 replicated more rapidly than RCAS (A), followed by a plateau at 4 d.p.i. in viral protein in cultured supernatant. Similarly, Sp-53 replicated in astrocytes showed more rapid replication than RCAS (A), with a peak at 7 d.p.i. in viral protein in supernatant (Figure 7c and 7d). Compared to DF-1, p27 of RCAS (A) was rarely detected in the supernatant of infected astrocytes. Antigen p27 and viral RNA were not detected in both control cells. Additionally, the mRNA levels of IL-1β were higher in Sp-53-infected astrocytes (the mean of mRNA level is 3.20 ± 0.49: calculated by the -ΔΔCt method by using *β-actin* as an internal control, n = 2) than in RCAS (A)-infected cells (0.52 ± 0.12, n = 2) at 9 d.p.i..

Discussion

Fowl glioma is defined as multiple nodular growths of astrocytes with disseminated non-suppurative encephalitis. In this chapter, the relationship between intracerebral viral replication and astrocytic growth in the early infection phase was investigated. Among the C/O SPF chickens inoculated *in ovo* with three different titres of Sp-53 (a FGV variant), chickens with higher titres revealed multiple proliferation of astrocytes and the

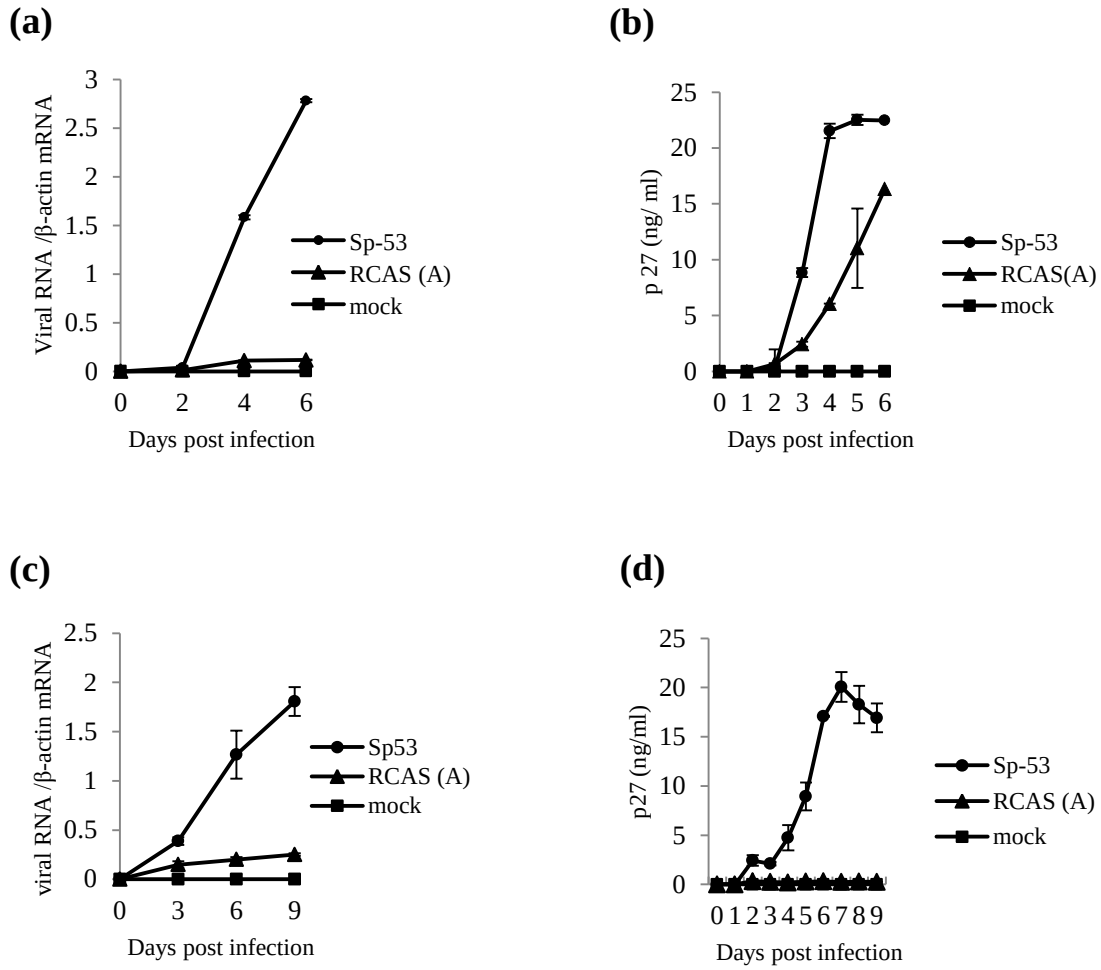

Figure 7. Viral replication in cultured cells. (a) Viral RNA levels of DF-1 infected with Sp-53 and RCAS (A). (b) Antigen p27 in cell supernatant of DF-1 infected with Sp-53 and RCAS (A). (c) Viral RNA levels of primary astrocytes infected with Sp-53 and RCAS (A). (d) Antigen p27 in cell supernatant of primary cultured astrocytes infected with Sp-53 and RCAS (A). Error bars represent the means ± standard error of the means (n=2).

levels of IL-1β in those brains were increased in close correlation with the viral load and intracerebral viral replication. Additionally, Sp-53 replicated more quickly and at higher titres than RCAS (A) in DF-1 cells and primary cultured astrocytes and enhanced the excessive release of IL-1β from the infected astrocytes.

The level of viral antigen is not always correlated with neurological disease progression associated with retroviruses, including HIV-1, HTLV-1 and SIV. In macaque with SIV, a high viral load in cerebrospinal fluid and brain tissue could be predictive of the development of CNS lesions associated with these viral infections (Zink *et al*., 1999: Dang *et al*., 2012). On the other hand, some affected individuals showed no correlation between CNS lesions and CSF viral load (Matsuda *et al*., 2013). In the current study, the positive correlation between intracerebral viral load and degree of astrocytic growth was recognised in the early infection phase, indicating that the inflammatory response to viral infection is dominant in this phase.

The levels of IL-1β were correlated with intracerebral viral RNA levels of Sp-53 in the experimental infection and cultured astrocytes infected with Sp-53 excessively released this proinflammatory cytokine following successful viral replication. IL-1β affects cell proliferation and the survival of neoplastic astrocytes via NF-κB, p38/MAPK and JNK pathway (Sen, 2011; Yeung *et al*., 2013). Activated astrocytes themselves produce IL-1β and enhance its effects in an autocrine and paracrine manner (Yamanaka *et al*., 1994). In addition, IL-1β induces reactive astrocytic proliferation as a response to virus itself and/or viral cytopathic effects in viral infections. Specifically, highly pathogenic avian influenza virus induces IL-1β and IL-6 secretion from activated macrophages and lymphocytes, resulting in systemic cytokine storm and finally death of chickens (Wang *et al*., 2008). HIV-1 up-regulates IL-1β in the brain with HIV

encephalitis and IL-1β is expressed mostly by CD68-positive macrophages/microglia and rarely by astrocytes (Xing *et al*., 2009). The production of mature IL-1β is associated with both pro-IL-1β expression and inflammasome activation. It is suggested that virus-productive infection, especially viral RNAs produced after the integration of proviral genome, can induce pro-IL-1β expression and activate the inflammasome in HIV-1 infection (Guo *et al*., 2014). Like mammalian IL-1β, Chicken IL-1β contains an NH2-terminal pro-domain (Jobling *et al*., 1988), and chicken orthologue of caspase-1 has been already cloned (Johnson *et al*., 1998). These facts suggest that a mechanism for chicken IL-1β maturation similar to that in mammals may be used (Gibson *et al*., 2014). At the same time as IL-1β release, cytopathic effects and cell cycle arrest can occur in avian influenza virus and HIV-1 infection. Avian influenza viruses trigger the direct cellular damage resulting in necrosis (Ng *et al*., 2010), whereas HIV-1 accessory protein, Vpr, can cause cell cycle arrest in the infected cells (Ayyavoo *et al*., 1997). However, there are limited manifestations on ALV-A infection, although TGF-β2 expression has been reported to be up-regulated in the serum of infected chickens (Barbour *et al*., 1999). Sp-53 had higher replication ability in cultured astrocytes and induced excessive release of IL-1β from these cells, suggesting that IL-1β was produced by the astrocyte response to viral infection and excessive viral replication. Furthermore, ALV-A has the simplest genome structure without any accessory genes and shows no cytopathic effects in the infected cells. Therefore, ALVs showing high replication ability in chicken astrocytes could induce the glial cells to release IL-1β, which affects astrocytic growth through an autocrine/paracrine signal pathway.

TGF-β is a multipotent cytokine that can regulate cell growth, differentiation, apoptosis and development (Ten Dijke & Hill, 2004; Rahimi & Leof, 2007). TGF-β

promotes the proliferation of fibroblasts, whereas it inhibits the proliferation of blood cells and epithelial cells (Jackowlew, 2006; Hill *et al*., 2009). Although the effects of TGF-β on astrocytic growth are still controversial, TGF-β could promote or inhibit the proliferation of astrocytes in several neoplastic diseases (Massagué, 2008; Tiwari *et al*., 2011). TGF-β can also induce self-renewal and oncogenic capability of one glioma cell line, LN-229, in cooperation with IL-1β, although the detailed molecular mechanism of the phenomenon is not clear. Thus, the intracerebral up-regulation of TGF-β in chickens inoculated with $5x10^4$ TCIU of Sp-53 implies that TGF-β as well as IL-1β may contribute to severe astrocytic proliferation in this group.

The LTR domain of ALVs, which is formed by the integration of viral cDNA in the S phase of mitosis, performs a crucial role to induce avian lymphoid leukosis. When the provirus is eventually inserted upstream of cellular oncogenes, the LTR domain activates transcription of these genes, resulting in tumour formation (promoter insertion). Transformation of host cells usually takes more than 5 months in lymphoid leukosis. Although there is currently no reliable method to distinguish between reactive and neoplastic astrocytes in fowl glioma, the oncogenesis theory cannot explain the pathogenesis of fowl glioma because the gliomatous lesions are detected 35-70 days after *in ovo* infection in Chapter I.

In conclusion, these results demonstrate that astrocytic growth at least in the early phase of fowl glioma-inducing ALV infection could be promoted by autocrine/paracrine IL-1β production by astrocytes.

Summary

Fifty-seven FGV variants have been isolated from Japanese fowls so far and these variants have a variable degree of glioma-inducibility. However, how these ALVs induce glioma with different degrees and frequencies has not been fully elucidated. In this chapter, the relationship between intracerebral viral replication and astrocytic growth in the early infection phase was investigated. Replication abilities of two ALV strains, Sp-53 (a FGV variant) and replication-competent ALV-based vector RCAS (A) without glioma-inducibility, were compared in the brains of C/O SPF chickens at 35 days of age. Sp-53 replicated faster than RCAS (A), and the histological score and the level of IL-1β in brains increased depending on the level of intracerebral viral RNA. Up-regulation of IL-1β was also demonstrated in primary cultured astrocytes. These results suggest that the astrocytic growth in this phase is enhanced through the autocrine/paracrine production of IL-1β in the FGVs-infected astrocytes.

Chapter III

Congenital cerebellar dysplasia in White Leghorn chickens (*Gallus gallus domesticus*)

Introduction

Congenital cerebellar anomalies are common in domestic animals and are classified into hypoplasia, abiotrophy and dysplasia (Maxie & Youssef, 2007). Cerebellar hypoplasia secondary to an *in utero* or perinatal viral infection is most commonly seen in domestic animals, including cats, cattle and pigs. Cerebellar abiotrophy refers to premature or accelerated degeneration of formed elements, presumably caused by some intrinsic metabolic defect. Cerebellar dysplasia is a rare entity in domestic animals with the exception of mouse cerebellar mutants studied in developmental biology (Rice & Curran, 1999). The cerebellar disorder has been described as a part of Dandy-Walker syndrome, Arnold-Chiari malformation, copper deficiency in sheep and some metabolic storage disorders, although minor dysplastic lesions of no consequence are common in young animals (Maxie & Youssef, 2007). In contrast to mammals, congenital cerebellar abnormalities have been rarely reported in birds. Cerebellar hypoplasia due to viruses, including a chicken parvovirus, ALVs and an Aino virus, has been previously described (Kitano *et al*., 1997; Toyoda *et al*., 2006; Marusak *et al*., 2010). Cerebellar hypoplasia, suspected of being a genetic disorder, has also been described in two free-living American kestrels (Armién *et al*., 2013). Here, the morphological characteristics of cerebellar dysplasia were described in SPF White Leghorn chickens.

Materials and methods

Animals

Seven chickens examined in this study were prepared as control animals for experimental infection of some avian leukosis virus. Fertile eggs of a SPF White Leghorn strain were purchased from a commercial vendor. All eggs were incubated at 37.5°C and inoculated via the yolk sac on the sixth day of incubation with 0.1 ml of culture medium without any pathogen. Culture medium was Dulbecco's modified eagle medium (Nissui Pharmaceutical Co., Tokyo, Japan) added with 3,500 mg/l D (+)-glucose (Wako Pure Chemical Industries Ltd., Osaka, Japan) and 4 mM L-glutamine (Life Technologies). The hatched chicks were reared in isolators in the animal facilities of Hokkaido University, and euthanized at 0 and 35 days of age. The chickens did not receive any vaccinations or medication. All experiments were performed humanely according to the guidelines set by the Animal Care and Use Committee of Graduate School of Veterinary Medicine, Hokkaido University (Permission number: 1148).

Histopathology and immunohistochemistry

The brain and other organs, including the liver, spleen, kidneys, heart, lungs, bone marrow, gastrointestinal tract, bursa of Fabricius, thymus, spinal cord, peripheral nerves and skeletal muscles, were fixed in neutral-buffered 20% formalin, embedded in paraffin wax, sectioned at 4 μm thickness, and examined by light microscopy after staining with haematoxylin and eosin. Bodian stain was also performed to visualize axon of Purkinje cells.

For the immunohistochemical examination, selected sections were deparaffinised. The sections for vimentin evaluation were pretreated with trypsin (0.1% in 0.1 M Tris buffer) for 30 minutes at 37°C and other sections for GFAP and proliferating cell

nuclear antigen (PCNA) were pretreated with microwave. The sections were treated with 0.3% hydrogen peroxide to inhibit endogenous peroxidase. Indirect immunoperoxidase staining was performed using a commercial streptavidin-biotin kit (Nichirei Corp.). After the blocking of nonspecific reactions, each section was incubated with specific primary antibodies: against vimentin (1:100, clone Vim3B4, Dako), GFAP (1:2,500, Dako) or PCNA (no dilution, Dako).

Immunofluorescence and confocal microscopy

Sections were cut at 10 μm, deparaffinised and washed twice with phosphate-buffered saline (pH 7.4) containing 0.1% Triton X-100 (PBST) and blocked with 2% bovine serum albumin (BSA) in PBST for 30 minutes. A rabbit polyclonal anti-calbindin D28 antibody (1:400, Spring Bioscience, CA, USA) and a mouse monoclonal anti-vimentin antibody (1:100, clone 3B4, Dako) were used and incubated at 4°C overnight in a humidified chamber. Following three washes in PBST, bound antibodies were detected with Alexa488-conjugated donkey anti-rabbit and Alexa555-conjugated donkey anti-mouse immunoglobulin G (Life Technologies). After three additional washes in PBST, coverslips were mounted with ProLong Gold with bisBenzimide H 33258 (Sigma-Aldrich, St Louis, MO, USA) and images were acquired with a Zeiss LSM-700 confocal microscope (Carl Zeiss Microscopy GmbH, Jena, Germany).

Polymerase chain reaction

PCR was conducted on DNA extracted from frozen brain tissue for ALVs, Marek's disease virus serotype 1 and chicken parvovirus as described previously (Chang *et al.*,

2002; Hatai *et al*., 2005; Zsak *et al*., 2008; Tarasiuk *et al*., 2012). The PCR products were electrophoresed through 1.5% agarose gels.

Results

All seven SPF chickens showed no clinical signs. At necropsy, cerebellar folia grossly showed an irregular disorganized pattern in four and three chickens at 0 and 35 days of age, respectively (Table 5 and Figure 8a). Both males and females were affected. The size of the affected cerebellums appeared normal. Common histopathologic findings in these cerebellums were solitary or multiple cerebellar cortical tissue islands from deeper cortices to the medulla of the vermis (Figure 8b). These ectopic cortical tissues consisted of tangled islands of molecular and granular cell layers with haphazardly distributed Purkinje cells (Figure 8c), although the cortical layers other than the lesions remained in correct order. The small, round to spindle cells with round to oval nuclei and scant cytoplasm, which resembled granular cells, also aggregated around small vessels at one to three cells thick (Figure 8d). Mitotic figures were occasionally observed in these granular cells. The thickness of molecular and granular cell layers overlaying these ectopic tissues was slightly reduced and external granular cell layers were one to two cells thick.

In sections stained by Bodian's method, heterotopic Purkinje cells intermingled with numerous disorganized axonal processes. By using immunofluorescence analysis for calbindin and vimentin, Purkinje cells in both the heterotopic islands and the cortex with normal structure were strongly positive for calbindin D28 protein. The heterotopic

Table 5. Distribution and degree of cerebellar dysplasia in SPF chickens.

No.	Age (day)	Sex	Distribution	Location	Degree
1	N[a]	Male	Focal	vermis	very mild
2	N	Male	Focal	vermis	Severe
3	N	Male	Multifocal	vermis	Severe
4	N	Female	Multifocal	vermis, right flocculus	Severe
5	35	Male	Focal	vermis, left flocculus	Severe
6	35	Female	Focal	vermis	Mild
7	35	Female	Multifocal	vermis	Moderate

[a] Neonatal chick.

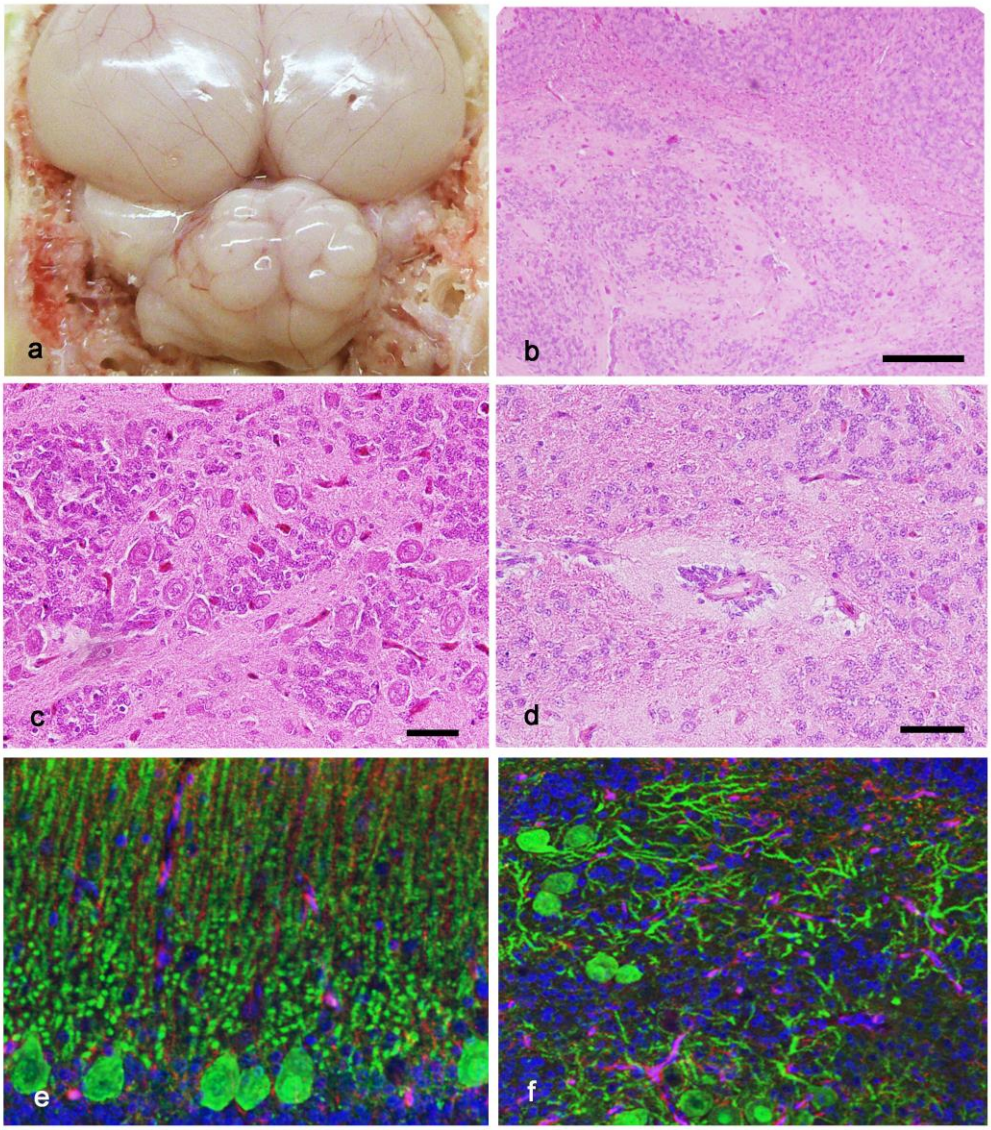

Figure 8. Gross, microscopic features and immunofluorescence in the cerebellum of chickens. a: Disorganization of cerebellar folia. Chicken No. 7. b: Heterotopic cortex located from granular layer to medulla. Chicken No. 1. Haematoxylin and eosin stain. Bar = 100 μm. c: Disarrangement of cortical components in heterotopic cortex. Chicken No. 4. Haematoxylin and eosin stain. Bar = 40 μm. d: Aggregation of granular cells around vessel. Chicken No. 7. Haematoxylin and eosin stain. Bar = 40 μm. e: Vimentin-positive Bergmann's glia (red) and calbindin D28-positive dendrites of Purkinje cells (green) grow straight toward the meninges in normal cortex. Immunofluorescence. f: Radiated dendrites of Purkinje cells (green) with few Bergmann's glia fibres (red) in heterotopic cortex. Immunofluorescence.

Purkinje cells randomly extended dendritic processes into the adjacent tissue and formed a molecular layer-like structure. A few vimentin-positive Bergmann's fibres were disordered in the ectopic tissues, whereas the fibres radially extended toward the pial surface from the Golgi epithelial cells (Bergmann's glia) in the normal cortex (Figure 8e and 8f). The granular cells that aggregated around vessels were positive for PCNA. All cells within the ectopic tissue were negative for GFAP.

The cells in the affected brains were negative for ALVs, Marek's disease virus and chicken parvoviruses by PCR.

Discussion

All examined birds developed single to multiple heterotopic cerebellar cortexes from the deeper cortex to the medulla, mainly in the vermis. These heterotopic tissues consisted of disordered molecular, Purkinje cell and granular cell layer components.

The classification of cerebellar abnormalities appears to be confusing in veterinary medicine (Maxie & Youssef, 2007). In veterinary fields, cerebellar abnormalities are divided into two broad categories, namely, hypoplasia and abiotrophy. In addition to these two categories, cerebellar dysplasia has been reported to be a minor entity and common in young animals rather than in adults. It has been most commonly detected in the flocculonodular lobules in mammals. The foci are histopathologically characterized by tangled islands of germinal, molecular and granular cell layers with Purkinje cells distributed haphazardly. Such dysplasia is reported as part of the abnormalities of

Dandy-Walker syndrome, Arnold-Chiari malformation, copper deficiency of sheep and metabolic storage disorders. On the other hand, more detailed classifications for cerebellar dysplasia, including cerebellar heterotopia as one of the types of isolated hemispheric dysplasia, are proposed in human medicine (Patel & Barkovich, 2002; Ellison *et al*., 2004). According to the classifications, cerebellar heterotopias fall into one of the dysplastic categories and are morphologically characterized by heterotopic grey matter within the cerebellar white matter. The foci are incidentally found in the hemispheres of infants, varying from a few cells to large islands of grey matter in which there are clusters of large cells surrounded by neuropil or islands of heterotopic cortex. On the basis of the classification of human medicine, the lesions of the current cases were consistent with cerebellar heterotopia because the cerebellar cortical tissues with disordered layers were distributed in the cerebellar medulla, which resulted in disarrangement of folia. In contrast to human cerebellar heterotopia, the ectopic islands in the current cases were mainly located in the vermis. This is considered to reflect the anatomical difference between mammal and chicken cerebellum as the lateral lobes of the cerebellum in avian species are rudimentary and small in size. Although the thickness of the molecular and granular cell layers overlaying the ectopic tissues were slightly reduced, these foci seemed to be too small to cause cerebellar signs in these affected chickens.

The two most common causes of congenital cerebellar abnormalities in domestic animals are (1) hypoplasia and atrophy secondary to an *in utero* or perinatal viral infection and (2) a primary developmental defect malformation. The former most commonly occurs in cats and cattle (Maxie & Youssef, 2007), but has on rare occasions been reported in birds infected with avian parvovirus (Marusak *et al*., 2010), one strain

of avian leukosis viruses (Toyoda *et al*., 2006) and Aino virus (an arthropod-borne virus of Bunyaviruses) (Kitano *et al*., 1997). Those abnormalities are characterized by a smaller cerebellum and histopathologically thinned granular cell layer and disorganized Purkinje cells with selective necrosis of granular cells and gliosis. In the present cases, cerebellums had neither necrosis of the nervous tissues nor gliosis and all seven chickens were negative for chicken parvoviruses and ALVs by PCR. These results suggest that the cerebellar dysplasia in this study is likely to be genetic in cause. However, there seems to be no additional occurrence of these cerebellar lesions in this chicken strain after generational change.

There is only one report on cerebellar hypoplasia as a primary developmental defect malformation in avian species (Armién *et al*., 2013). In this previous report, the authors describe Purkinje cell heterotopy with cerebellar hypoplasia in two free-living American kestrels and that the anomaly seems to be genetically induced by molecular disruption of Purkinje cell migration, placement and maturation.

Development of the cerebellum is a complex event involving a number of cell types and this event is regulated by gradual gene expression (McGeady *et al*., 2006). Therefore, numerous gene abnormalities have been reported to contribute to the pathogenesis of cerebellar dysplasia in laboratory animals (Wang & Zoghbi, 2001). In the development process of the cerebellum in chick embryos, Purkinje cells and Bergmann's glia originate in the rhombic lip and migrate to form an irregular layer from the 3rd to the 6th day of incubation (Nickel *et al*., 1973; Akar & Sur, 2010). At this stage, Purkinje cells move from the rhombic lip to their future position along radial fibres with the guidance of Reelin secreted from external granular cells. The external granular cell layer is formed between the 6th day and 15th day of incubation. The

granular cells of the external granular cell layer migrate through the molecular layer to form the internal granular cell layer from the 18th day of incubation, peak at 2 days of age and are finally complete around 34 days of age. Bergmann's fibres act as guides for the migration of granular cells during this process. Genetic defects, including mutation within *math1* and *reln*, have been reported to induce Purkinje cell heterotopy and disorganization of the cerebellar cortex architecture in mice (Heckroth *et al*., 1989; Jensen *et al*., 2002). Over 95% of Purkinje cells are ectopic in the *reeler* mutant mouse because of complete loss of the Reelin signal, whereas one population of Purkinje cells was located in an aberrant position in *math1* null-mutant mouse due to the lack of an external granular cell layer. As well as Purkinje cell heterotopy, anomalies in the folia and fissures have been suggested to be associated with defects of genetic controls in the foliation process (Cerri *et al*., 2010). Bergmann's glial fibres direct migration of the granular cells at the base of fissure and the Purkinje cells regulate the number of folia by secreting sonic hedgehog, which influences granular cell proliferation in the external granular cell layer (Corrales *et al*., 2006; Sudarov & Joyner, 2007). It is suggested that the genetic defects change the relationship among glial fibre morphology, granular cell migration and Purkinje cell differentiation and impede the mechanical forces of foliation, resulting in alteration of cerebellar architecture (Cerri *et al*., 2010). The condition in our cases was likely due to defects of radial glia fibres and related migration factors. This is the first report on cerebellar dysplasia in White Leghorn chickens (*Gallus gallus domesticus*).

Summary

Congenital cerebellar anomalies have been rarely reported in birds. In this chapter, cerebellums with disorganized folia in seven specific-pathogen-free White Leghorn chickens (*Gallus gallus domesticus*) were examined to clarify the relationship between them and ALV infection. Islands of heterotopic cortex were distributed from deeper cortices to the medulla in the cerebellum. The characteristic lesions were composed of randomly admixed components of the cerebellar cortex, including soma of Purkinje cells, dendrites of Purkinje cells in the molecular layer and granular cells. These characteristics of the lesion were quite different from ALV-induced cerebellar lesions. Immunofluorescence analysis revealed dendrites of Purkinje cells that extended haphazardly and a lack of Bergmann's glial fibres in the foci. Chicken parvovirus and ALVs were not detected in the affected birds by PCR. From histopathology and the lack of evidence for ALV infection, these cases are distinguished from ALV-induced cerebellar hypoplasia. This is the first report to indicate cerebellar dysplasia possibly caused by genetic abnormality in chickens.

Chapter IV

Cardiac pathology in avian leukosis virus infection

Introduction

Epidemiological studies (Roldan *et al*., 1987; Jacob *et al*., 1992; De Castro *et al*., 1994) have indicated that the risk of dilated cardiomyopathy and non-suppurative myocarditis rises in human patients infected with HIV-1. As experimental evidence in non-human primates, non-suppurative myocarditis and dilated cardiomyopathy with myocardial hypertrophy have been described in rhesus monkeys infected with SIVs (Shannon *et al*., 2000). These may occur as a result of the retrovirus itself acting either directly or indirectly via immunological mechanisms, opportunistic infection of other cardiotropic viruses or a combination of these mechanisms (Roldan *et al*., 1987; Jacob *et al*., 1992; De Castro *et al*., 1994; Shannon *et al*., 2000). Vpr of HIV has been recently suggested to be a unique polypeptide that causes atrial cardiomyocyte mitosis, mesenchymal tumour and dysrhythmia in the heart of transgenic mice with Vpr (Lewis *et al*., 2005). However, the information on the real cause and pathogenesis of retrovirus-induced cardiac disorders is limited.

In animals other than humans and non-human primates, Maedi-Visna virus from the genus *Lentivirus* and subfamily *Orthoretrovirinae* induces primarily lymphocytic inflammation in the heart of sheep, but no alteration of cardiomyocytes (Brellou *et al*., 2007). In avian species, myocarditis associated with ALVs has been reported in chickens (Gilka & Spencer, 1990; Gilka *et al*., 1991; Iwata *et al*., 2002). The myocarditis induced by ALV-A has been considered to be associated with excessive viral replication in cardiomyocytes (Gilka *et al*., 1991; Iwata *et al*., 2002). Additionally, dilated cardiomyopathy characterized by biventricular dilation and right ventricular hypertrophy has been described in chickens congenitally infected with ALV-J (Stedman

& Brown, 2002). The authors speculated that the cardiomyopathy resulting from persistent high-level synthesis of viral products might usurp the cellular machinery and substrates in cardiomyocytes and Purkinje fibres. These reports imply that several strains of ALVs are pathogenic to terminally differentiated cardiomyocytes. The causal relationship, however, is not completely established and the pathogenesis remains unclear. In this chapter, unusual hypertrophy and mitosis of cardiomyocytes, the morphology of which has not been previously reported in chickens infected with ALV-A were described. In addition, the causal relationship and pathogenesis are discussed on the basis of the molecular characteristics of isolates and the results of a reproducibility experiment with isolates.

Materials and Methods

Animals

The chicken breeds used in this study are listed in Table 6. These fowls were collected from the chicken flocks in which ALVs are widespread. Feather pulps and cloaca swabs were collected from 18 Japanese native chickens and stored at -80°C until use. For histological examination, the chickens were euthanized humanely according to a procedure approved the Animal Care and Use Committee of Graduate School of Veterinary Medicine, Hokkaido University (Permission numbers: 1094 and 1148).

Histopathology and immunohistochemistry

The heart and other organs, including the liver, spleen, kidney, lung and brain,

Table 6. Clinical signs, gross findings and results of ALV isolation in chickens.

No.	Breed	Sex (M/F)	Gross findings	Viral isolation		Isolated strain
				Cloaca swab	Brain	
1	Japanese Bantam	M	Anaemia	+	ND	Km_5880
2	Japanese Bantam	M	Atrophy of comb	+	ND	Km_5960
3	Japanese Bantam	M	None	+	ND	Km_5622
4	Japanese Bantam	M	None	+	ND	Km_5967
5	Japanese Bantam	M	None	+	ND	Km_6042
6	Japanese Bantam	F	Emaciation	+	ND	Km_5623
7	Japanese Bantam	F	Emaciation	+	ND	Km_5625
8	Japanese Bantam	F	Yolk peritonitis	+	ND	Km_5968
9	Japanese Bantam	F	Renal cyst	+	ND	Km_6045
10	Japanese Bantam	F	None	+	ND	Km_5621
11	Japanese Bantam	F	None	+	ND	Km_5624
12	Japanese Bantam	F	None	+	ND	Km_5843
13	Japanese Bantam	F	None	+	ND	Km_5852
14	Japanese Bantam	F	None	+	ND	Km_5892
15	Japanese Bantam	F	None	ND	+	Km_5897
16	Japanese Bantam	F	None	+	ND	Km_6209
17	Sebright Bantam	F	None	ND	+	Km_5900
18	Kumamoto Long Tail	F	None	+	ND	Km_6039

M: male, F: female

+: positive, -: negative, ND: no data

were fixed in 20% neutral-buffered formalin, routinely processed as described in Chapter I and sections were stained with haematoxylin and eosin. Masson's trichrome staining was performed in order to score myocardial fibrosis. Immunostaining using the labelled streptavidin-biotin method (Nichirei Corp.) was performed. The primary antibodies used were polyclonal antibody against ALV common antigens (1:5,000, courtesy of Dr. K. Tsukamoto, Azabu University, Japan) and monoclonal antibodies against avian reovirus (ARV) p17 antigen (1:50, Genesis Biotech Inc., Taipei, Taiwan), PCNA (no dilution, DAKO), phosphorylated Akt (p-Akt) (1:100, Cell Signaling Technology, MA, USA) and phosphorylated tuberin (p-tuberin) (1:100, Cell Signaling Technology).

RNA extraction and cDNA synthesis

Total RNA was extracted from brains, kidneys and hearts using TRIzol reagent (Life Technologies). Reverse transcription was performed as described in Chapter I. As an internal control for RNA extraction and cDNA synthesis, PCR amplification was performed for all cDNA samples using primers specific to chicken β-actin. The PCR for chicken β-actin was performed according to conditions described in Chapter I.

PCR amplification

Two types of PCR amplification were carried out with cDNA using primer sets. To detect the ALV genome, ALV-specific PCR was performed with a primer set of ALV #38 and ALV #39 (Table 1 in Chapter I). To detect the ARV genome, PCR for the S2 and S4 regions of ARV was performed with the primer sets of ARV sense primer (S2); 3'- CCC ATG GCA ACG ATT TC-5' and ARV antisense primer (S2); 3'- TTC GGC

CAC GTC TCA AC-5', and ARV sense primer (S4); 3'- GTG CGT GTT GGA GTT TC-5' and ARV antisense primer (S4); 3'-ACA AAG CCA GCC ATG AT-5', respectively, using a procedure previously described with some modification (Motitschke *et al*, 2010). The PCR mixture was a 10 μl reaction volume containing 1 μl of 10x *Ex Taq* Buffer (TaKaRa Bio), 0.8 μl of dNTP mixture, 2.5 mM each dNTP (TaKaRa Bio), 5 pmol each primer, 0.25 U *TaKaRa Ex Taq* HS (TaKaRa Bio) and 10 ng DNA. Touchdown PCR was performed, starting with denaturation step at 94 °C for 1 min followed by annealing step in which temperature decreased in steps of 2 °C, from 60 °C down to 48 °C. Two cycles were performed at each annealing temperature. Thirty-five cycles were then carried out at 95 °C for 30 sec, 48 °C for 30 sec and 72 °C for 30 sec. Finally, a prolonged extension step was performed at 72 °C for 10 min. The PCR products were analysed by 2% agarose gel electrophoresis.

Virus isolation and identification

For virus isolation, the supernatants of cloaca swabs from 16 chickens and brain emulsions of other two chickens were inoculated with 80% confluent DF-1 cells. DF-1 cells were obtained from the American Type Culture Collection and cultured as described in Chapter I. Cells were harvested 7 days after inoculation and were collected at that time. Concentrated culture supernatant was prepared according to the methods described in Chapter I.

Sequence analysis and phylogenic analysis

The *env*SU regions of 15 strains isolated from field cases and the complete virus genome of Km_5892 were sequenced as previously described in Chapter I. Sequencing

was conducted by Dragon genomics Center (Mie, Japan). The complete genomic RNA (gRNA) of Km_5892 has been deposited in the DDBJ/GenBank (AB682778). The obtained sequences were analysed with the Clustal W 1.8.3 program on the DDBJ website (http://clustalw.ddbj.nig.ac.jp/top-j.html) and the NCBI BLAST program (http://blast.ncbi.nlm.nih.gov/Blast.cgi). Phylogenic trees based on nucleotide sequences of *env*SU and *pol* were constructed on the DDBJ website by the neighbour-joining method implementing the Kimura method using isolated virus and other ASLVs. The topological accuracy of the tree was estimated by the bootstrap method with 1,000 replicates.

Birds and experimental infection

Fertile eggs from SPF White Leghorn strain WL-M/O (C/O) chickens were obtained from Nippon Institute for Biological Science and used in experimental infection. Chicken embryos were inoculated via the yolk sac on the sixth day of incubation with 5 x 10^4 TCIU of Km_5666 or Km_5892 strain and were euthanized at 35, 70 and 140 days of age. Seven control chicken embryos belonging to the uninfected group were similarly inoculated with 0.1 ml uninfected tissue culture medium and were euthanized at 35 days and 70 days of age. The hatched chickens were reared humanely according to the guidelines set by the Animal Care and Use Committee of Graduate School of Veterinary Medicine, Hokkaido University (Permission No. 13046). No chickens received any vaccinations or medication.

Results

Clinical signs and pathology in Japanese native fowls

Eighteen Japanese native fowls were collected and examined. A low rate of egg laying was observed in four fowls and emaciation in two (Table 6). At necropsy, one bird each had a small renal cyst and egg yolk in the body cavity (yolk peritonitis). Other twelve fowls showed no apparent gross lesions. The main histopathological changes in hearts were lymphocytic myocarditis, matrix inclusion bodies in cardiomyocytes and Purkinje fibres, fibrosis and hypertrophy of cardiomyocytes with atypical nuclei (Figure 9a-d). These lesions were noted mainly in the left ventricular wall and the degree of severity varied (Table 7). Multifocal lymphocytic myocarditis with mild myocardial necrosis and mild to severe interstitial myocardial fibrosis were observed in all cases. These foci contained a small number of plasma cells and macrophages. Intracytoplasmic, round to oval, unstained to basophilic inclusions (matrix inclusion bodies) were detected in cardiomyocytes and Purkinje fibres of all cases (Figure 9e). Additionally, individual hypertrophied cardiomyocytes or small clusters of cardiomyocytes with atypical, large nuclei were observed in seven (39%) fowls and these cardiomyocytes occasionally contained matrix inclusion bodies. The atypical nuclei were frequently arranged in long chains (1-11/high-power field) in the cytoplasm, and mitotic figures were also observed in these cardiomyocytes. The degree of cardiomyocyte hypertrophy was not correlated to the degree of myocarditis and the frequency of matrix inclusion bodies in the cytoplasm (Table 7). Other eleven chickens had neither hypertrophied cardiomyocytes nor atypical nucleus. Ten (56%) of eighteen fowls developed gliomas

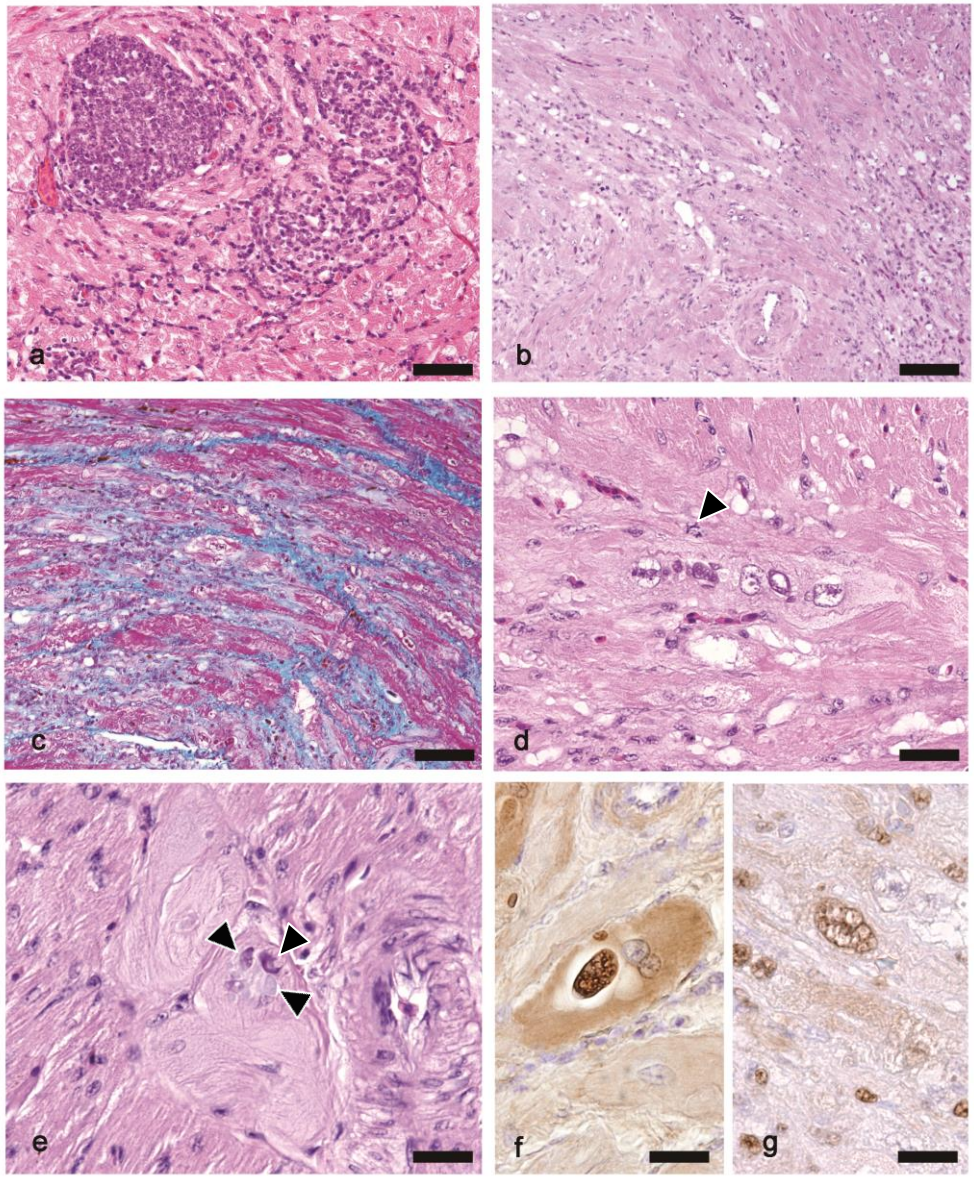

Figure 9. Histopathology and immunohistochemistry of hearts in Japanese native fowls. a: Mononuclear cells infiltrate into myocardial fibres. Chicken No. 5. Bar = 40 μm. b: Disarrangement of myocardial fibres with interstitial fibrosis. Chicken No. 9. Bar = 90 μm. c: Interstitial myocardial fibrosis confirmed by Masson's trichrome stain. Chicken No. 14. Bar = 25 μm. d: Hypertrophied cardiomyocytes with multiple atypical nuclei. Mitosis (arrowhead) is occasionally noted in these cardiomyocytes. Chicken No. 14. Bar = 20 μm. e: Matrix inclusion bodies (arrowhead) in the cytoplasm of Purkinje fibres. Chicken No. 14. Bar = 20 μm. f: Purkinje fibres and matrix inclusion bodies positive for ALV common antigen. Chicken No. 14. Bar = 20 μm. g: A large atypical nucleus in a hypertrophied cardiomyocyte is positive for PCNA. Chicken No. 14. Bar = 20 μm.

Table 7. The degree of cardiac lesions in field cases.

No.	Hypertrophied myocardium with atypical nucleus [a]	Non-suppurative myocarditis [b]	Fibrosis [c]	Matrix inclusion body [d]
1	-	+	+	109
2	+++	+++	+	39
3	-	++	+	7
4	-	++	++	99
5	-	+++	+	5
6	-	+	+	6
7	-	+	+	1
8	+	++	++	57
9	+	++	++	1
10	-	+	+	129
11	-	++	+	3
12	+	++	++	2
13	+	++	+	43
14	+++	+++	+++	27
15	-	+	+	49
16	-	+++	+	1
17	++	++	++	19
18	-	+++	++	12

[a] The degree of hypertrophied cardiomyocytes with atypical nuclei was defined as follows: +, individual cells; ++, multiple and/or small clusters; +++, multiple and extensive growth.
[b] The degree of non-suppurative myocarditis was defined as follows: +, focal or multifocal (under 25 μm in diameter); ++, multifocal (from 25 μm to 200 μm); +++, multifocal (over 200 μm).
[c] The degree of fibrosis was defined as follows: +, interstitial; ++, multifocal interstitial (under 400 μm in diameter); +++, multifocal interstitial (over 400 μm in diameter).
[d] Total number in 10 high-power fields.

in their brains. No significant lesion was observed in other organs of the examined cases, except for a renal cyst and yolk peritonitis grossly noted in one bird each. These cardiomyocytes, Purkinje fibres and matrix inclusion bodies were immunohistochemically positive for ALV common antigen (Figure 9f) and negative for avian reovirus (ARV) p17 antigen. Nuclei in hypertrophied cardiomyocytes were positive for PCNA (Figure 9g).

Viral isolation and polymerase chain reaction for ALVs and ARV

Feather pulps from all cases were positive for ALV-specific PCR and ALVs were isolated from cloaca swabs or brains of all affected chickens (Table 6). The hearts from 5 chickens (No. 2, 5, 9, 14 and 16), 2 chickens (No. 2 and 14) and the kidneys from other 13 birds were negative for ARV-specific PCR.

Phylogenic analysis of isolated ALV strains

The sequences of the *env*SU genes of sixteen strains isolated from the affected chickens were determined. The phylogenic analysis based on this region revealed that these strains could be classified into three clusters: MAV-1, FGV prototype and Km_ clusters (Figure 10). Five strains, including Km_5843, Km_5852, Km_5892, Km_5960 and Km_6045, isolated from fowls with hypertrophied cardiomyocytes belonged to two different clusters: FGV prototype and Km_ clusters. Next, the full-length genome of Km_5892, an isolate from the fowl with the most extensive distribution of hypertrophied cardiomyocytes was determined. The *env* gene of Km_5982 showed homology of 97% with that of FGV variant, Sp-40, and the 5'UTR, *gag-pol* and 3'LTR domains of Km_5982 showed 96%, 96% and 90% homology with those of TymS_90,

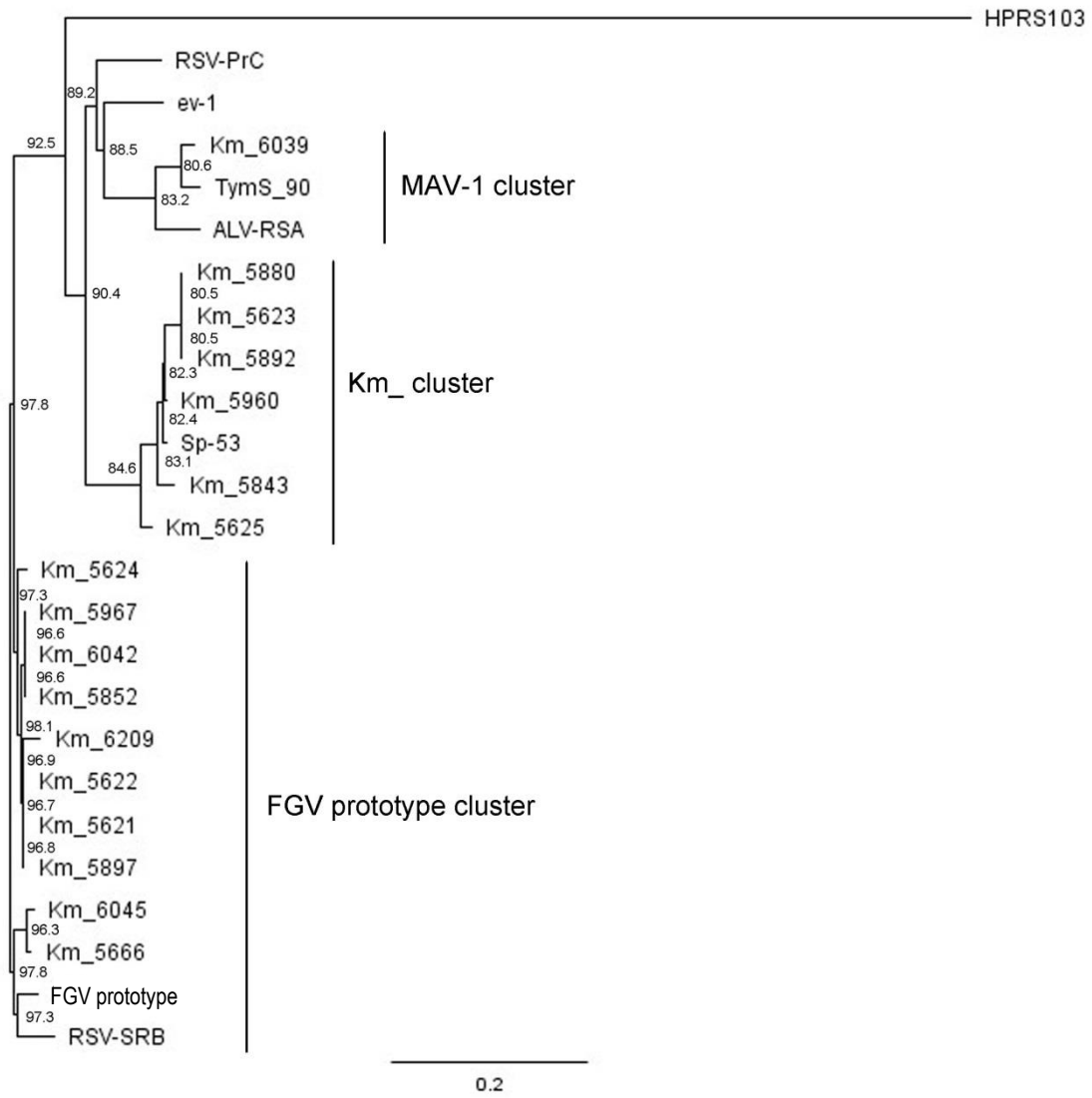

Figure 10. Phylogenic tree based on the *env*SU region of the isolates. Phylogenic tree constructed by the neighbour-joining method showing the relationships among the isolates, FGV prototype, Sp-53 (FGV variant) and standard ALSVs based on the SU region of the *env* gene. The amino acid sequences were aligned with the Clustal W 1.8.3 program. Bootstrap values of 1000 trials using the neighbour-joining method. Scale bar corresponds to a distance of 0.2 as the frequency of amino acid substitutions in the pairwise comparison of two sequences according to the Kimura two-parameter method.

respectively. Phylogenic analysis based on the *pol* gene revealed that Km_5892 could be classified into the same cluster as the other Km_ strains, including Km_5666, Km_5843 and Km_5845 (Figure 11). Km_5666 (accession number AB669896) is an ALV-A that was isolated from a Japanese Bantam kept in the same flock and the sequence of its full-length genome was previously analysed (Ochi *et al*., 2012a).

Pathology of chickens experimentally inoculated with Km_strains

Km_5666 and Km_5892 were picked up from two different clusters in phylogenic tree based on the *env*SU region of ALV and experimental infection using these two strains were performed. C/O SPF chicken eggs, inoculated *in ovo* with $5x10^4$ TCIU of Km_5666 and Km_5892 on the sixth day of incubation, were euthanized at 35, 70 and 140 days of age and examined pathologically (Table 8).

Paralysis of the left leg was observed in one of three (33%) Km_5666-inoculated chickens at 70 days of age. Other chickens showed no clinical signs. Multifocal lymphocytic myocarditis was observed in ten (83%) of twelve birds inoculated with Km_5666 and seven (100%) of seven with Km_5892. In these foci, lymphocytes and plasma cells admixed with a few macrophages and heterophils also infiltrated to various degrees. Hypertrophied cardiomyocytes with atypical nuclei were observed in two (17%) chickens with Km_5666 and one (14%) with Km_5892. One of the Km_5666-inoculated birds showed extensive multiple growths of atypical cardiomyocytes at 35 days of age (Figure 12a-c). Interstitial myocardial fibrosis associated with the inflammatory foci was observed in one (8%) Km_5666-inoculated chicken and two (29%) Km_5892-inoculated birds. Matrix inclusion bodies were detected in five (42%) and seven (100%) chickens inoculated with Km_5666 and

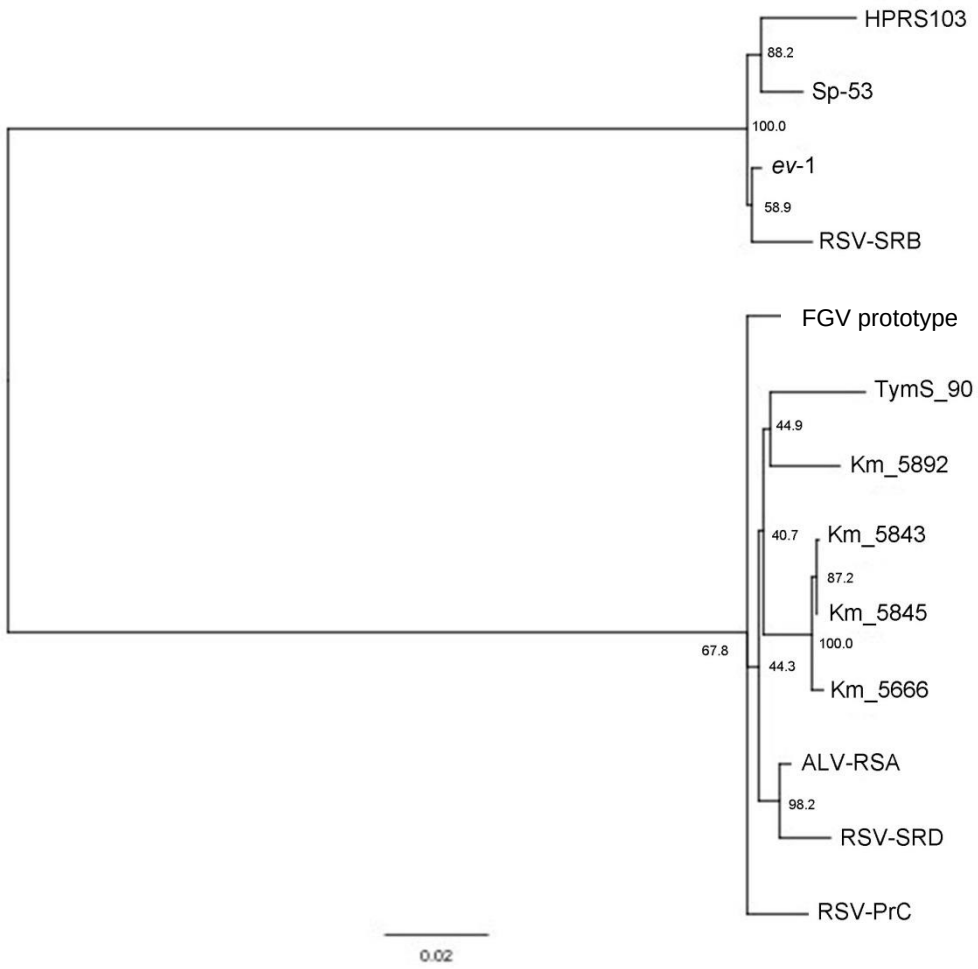

Figure 11. Phylogenic tree based on the *pol* gene of the isolates. Phylogenic tree constructed by the neighbour-joining method showing the relationships among Km_5892, FGV prototype and standard ALSVs based on the *pol* gene. The nucleotide sequences were aligned with the Clustal W 1.8.3 program. Bootstrap values of 1,000 trials using the neighbour-joining method. Scale bar corresponds to a distance of 0.03 as the frequency of amino acid substitutions in the pairwise comparison of two sequences according to the Kimura two-parameter method.

Table 8. The degree of cardiac lesions in chickens experimentally infected with Km_5666 and Km_5892.

Inoculated strain	Age (days)	N	Hypertrophied myocardium with atypical nucleus[a]				Non-suppurative myocarditis[b]				Fibrosis[c]		Matrix inclusion body[d]	
			-	+	++	+++	-	+	++	+++	-	+	-	+
Km_5666	35	6	5	0	0	1	2	3	0	1	6	0	5	1
	70	3	2	1	0	0	0	1	2	0	3	0	1	2
	140	3	3	0	0	0	0	1	2	0	2	1	1	2
Km_5892	35	4	4	0	0	0	0	2	2	0	3	1	0	4
	70	3	2	0	1	0	0	1	2	0	2	1	0	3

[a] The degree of hypertrophied cardiomyocytes with atypical nuclei was defined as follows: +, individual cells; ++, multiple and/or small clusters; +++, multiple and extensive growth.
[b] The degree of non-suppurative myocarditis was defined as follows: +, focal or multifocal (under 25 μm in diameter); ++, multifocal (from 25 μm to 200 μm); +++, multifocal (over 200 μm).
[c] The degree of fibrosis was defined as follows: +, interstitial; ++, multifocal interstitial (under 400 μm in diameter); +++, multifocal interstitial (over 400 μm in diameter).
[d] Total number in 10 high-power fields.

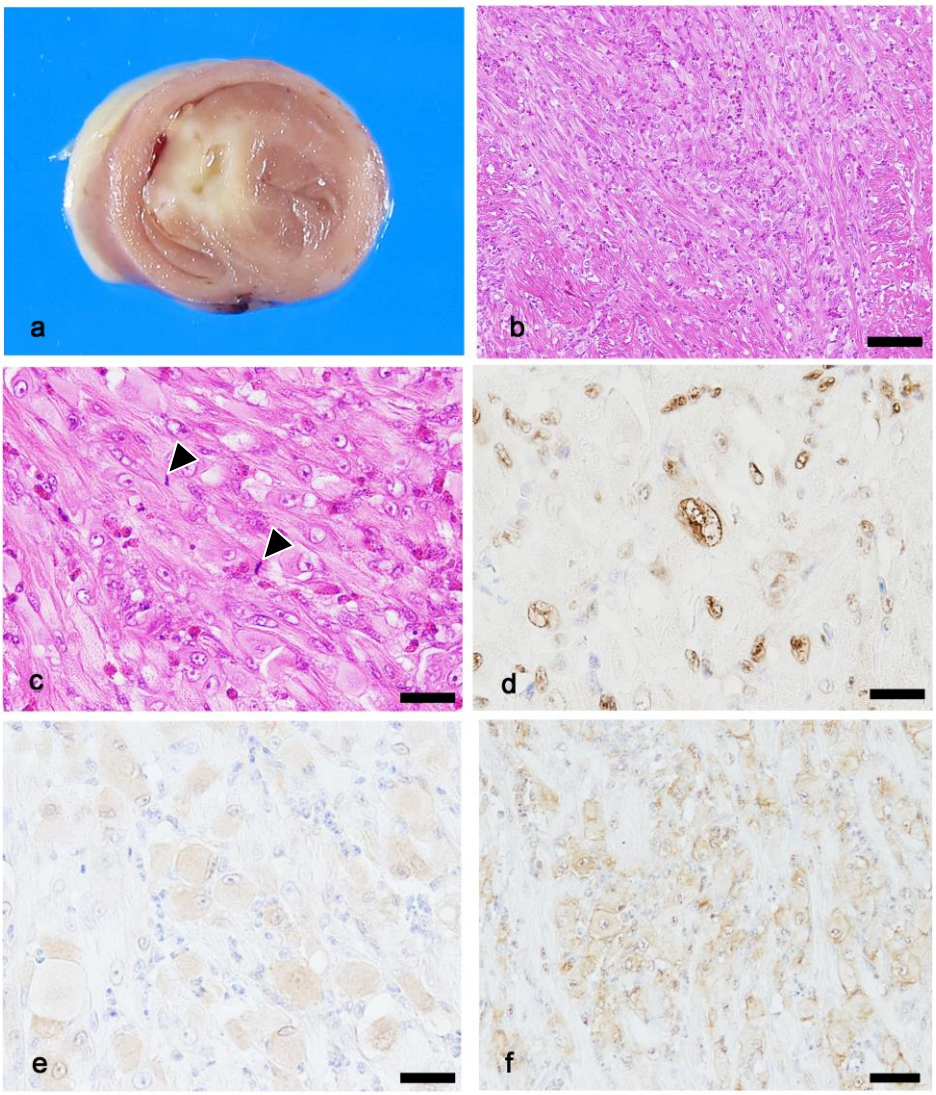

Figure 12. Gross pathology, histopathology and immunohistochemistry of chickens experimentally inoculated with Km_5666. a: Greyish-white ill-defined tissue was located in the septum at 35 days old. b: Locally extensive growth of hypertrophied cardiomyocytes. Haematoxylin and eosin stain. Bar = 75 µm. c: Mitosis (arrowhead) observed in hypertrophied cardiomyocytes. HE stain. Bar = 30 µm. d: Numerous nuclei in atypical myocardium were positive for PCNA. Streptavidin-biotin complex, haematoxylin. Bar = 20 µm. e-f: Hypertrophied cardiomyocytes positive for p-Akt (e) and p-tuberin (f). Streptavidin-biotin complex, haematoxylin. Bars = 20 µm.

Km_5982, respectively. In terms of immunohistochemistry, the cytoplasm of cardiomyocytes and Purkinje fibres and matrix inclusion bodies were positive for ALV common antigen and nuclei in atypical cardiomyocytes were positive for PCNA (Figure 12d). The cytoplasm of hypertrophied cardiomyocytes was also positive for p-Akt and p-tuberin (Figure 12e and 12f). By using RT-PCR and sequencing, the hypervariable regions of Km_5666 and Km_5982 were detected from the brain and heart of inoculated birds, respectively. No significant lesion was observed in the control birds inoculated with medium.

Discussion

The cardiac lesions of native fowls were histologically characterized by atypical hypertrophied cardiomyocytes with mitosis and non-suppurative myocarditis. ALVs were isolated from all affected cases and similar cytological changes were reproduced by experimental infection with Km_5666 and Km_5982. In addition, extensive multiple growths of atypical cardiomyocytes were also recognized in a Km_5666-inoculated bird. These results demonstrate that ALVs can cause atypical hypertrophied cardiomyocytes and mitosis and on rare occasions induce extensive growth. The distribution and cytological features of cardiomyocytes clearly differed from those of physiological cardiac hypertrophy and those of idiopathic primary myocardial diseases, including human and feline cardiomyopathies (Schoen & Mitchell, 2004; GrantMaxie & Robinson, 2007; Miller *et al*., 2012). Such individual and/or massive hypertrophy of cardiomyocytes has not been previously reported in any avian disease, except for in one

chicken experimentally infected with FGV prototype (Tomioka *et al*., 2003).

ARV causes a cardiac abnormality grossly characterized by right atrial dilation and microscopically non-suppurative myocarditis with multifocal necrosis and multinuclear giant cell formation (Shivaprasad *et al*., 2009). However, ARV infection occurs mainly in turkeys rather than in chickens, and the histological changes were easily differentiated from those of our cases, especially on the basis of atypical hypertrophy of cardiomyocytes. In addition, cases in this study were immunohistochemically negative for ARV p17 antigen and negative for ARV S2 and S4 genome by PCR.

Cardiac rhabdomyomas are often found incidentally in human infants affected by tuberous sclerosis (Benyounes *et al*., 2012) and in swine juveniles (Tanimoto & Ohtsuki, 1995), and are considered as a malformation or a hamartoma rather than a true neoplasm (Schoen & Mitchell, 2004; GrantMaxie & Robinson, 2007; Miller *et al*., 2012). Rhabdomyomas are morphologically characterized by multiple nodules composed of enlarged cardiomyocytes with a distinct border and the appearance of "spider cells", which are defined as large cardiomyocytes with numerous vacuoles in their cytoplasm due to glycogen accumulation. In contrast, their malignant counterpart, rhabdomyosarcoma, is quite rare in avian species and there has been just one report of rhabdomyosarcoma induced by the MC29 strain (Beard, 1980; Saule *et al*., 1987), which is a replication-deficient avian myelocytomatosis virus with v-*myc* oncogene and belongs to the group of acutely transforming viruses. Morphologically, rhabdomyosarcoma is characterized by the proliferation of large vacuolated cardiomyocytes with severe cellular and nuclear atypia and shows invasive growth. Hypertrophied cardiomyocytes showing extensive growth in a Km_5666-inoculated bird had glassy cytoplasm with a few vacuoles. Although these morphological features

were different from those of naturally occurring cardiac neoplasms, the cardiac lesions consisting of atypical cardiomyocytes in a Km_5666-inoculated chick (35 days of age) were considered to be in the category of hamartoma.

ALVs show high tropism to myocardial fibres and matrix inclusion bodies, which are composed of ribosomes and immature virions that accumulate, are frequently formed in association with ALV replication in infected cardiomyocytes (Gilka & Spencer, 1985; Nakamura *et al.*, 1988; Hafner *et al*., 2007). Non-suppurative myocarditis was found to occur in experimental cases with some ALV strains, including RAV-1 and 7 (Heidrich *et al*., 1987; Gilka & Spencer, 1990) and these inflammatory changes are interpreted as being induced by viral replication in cardiomyocytes. On the basis of these findings, four possible mechanisms are considered to explain the ALV-induced cardiomyocyte hypertrophy in the present study. First, these lesions may develop as reactive changes secondary to non-suppurative myocarditis. The frequency of hypertrophied cardiomyocytes, however, was not correlated with the degree of myocarditis. It seems unlikely that the abnormal cardiomyocytes are merely a reactive change. Second, the lesions may develop due to physical stimuli of matrix inclusion bodies. Hypertrophy of myocardial fibres is known to be induced by the formation of matrix inclusion bodies (Stedman & Brown, 2002). However, there are no findings that atypical large nuclei and mitosis develop in association with the formation of matrix inclusion bodies in any previous reports on ALV-infected heart. Third, the formation of atypical cardiomyocytes may be associated with promoter insertion of ALV (Maeda *et al.*, 2008). However, transformation of host cells usually take more than 5 months in avian lymphoid leukosis by ALV-A because multiple rounds of infection must occur in an infected animal before a provirus inserts itself in the vicinity of a cellular

proto-oncogene with appropriate activation. Promoter insertion cannot explain the development of cardiomyocyte hypertrophy and hamartoma in 35-day-old birds in this study. Three oncogenic mechanisms of retroviruses other than promoter insertion are known: 1) transformation by viral oncogenes, 2) oncogenesis by accessory proteins such as Tax of HTLV-1 and 3) envelope protein-induced transformation (Maeda *et al*., 2008). The viral genomes of Km_5666 (Ochi *et al*., 2012a) and Km_5892, however, contain neither a viral oncogene nor any genes coding accessory proteins. The last possible mechanism is that viral components such as envelope proteins may cause signaling pathway abnormality in host cells, resulting in a change of cellular function and morphology (Maeda *et al*., 2008). Recently, Jaagsiekte sheep retrovirus (JSRV) has been reported to cause transformation of host cells by its transmembrane envelope domain (Zavala *et al*., 2003; Hull *et al*., 2012). Envelope protein of JSRV involves the PI3K/Akt pathway in transformation (Zavala *et al*., 2003). Once the PI3K/Akt pathway is activated, cellular genes associated with protein synthesis, proliferation and survival are up-regulated. Among these genes, tuberin and mammalian target of rapamycin (mTOR) are known to have a crucial role in the proliferation and hypertrophy of cells (Dorn & Force, 2005). Dephosphorylated tuberin (activated form) was shown to regulate cellular status by suppressing the mTOR activator, Rheb. In the presence of stimulation, p-Akt suppresses the activation of tuberin by phosphorylation, resulting in cellular hypertrophy and proliferation. Immunohistochemical results on p-tuberin and p-Akt in this study suggest that hypertrophy and proliferation of cardiomyocytes may be caused by activation of the mTOR signaling pathway.

The *env* gene and LTR are mainly involved in the tumorigenesis of ALVs. A previous study indicated that the *env* gene of Km_5666 is very similar to the FGV

prototype, whereas other regions of this strain, including 5'UTR, *gag-pol*, 3'UTR and 3'LTR, show high homology with TymS_90 (Ochi *et al*., 2012a). On the other hand, the *env* gene of Km_5892 was found to be closely related to that of a FGV variant (Sp-40), whereas other regions, including 5'UTR, *gag-pol* and 3'LTR, were shown to be similar to those of TymS_90. Km_5666 and the other isolates from birds affected by cardiomyocyte hypertrophy in the current study belonged to two clusters in the phylogenic analysis based on the *env*SU region. These results suggest that there is genetic diversity among ALVs showing the inducibility of cardiomyocyte hypertrophy, implying a high prevalence of cardiac abnormality among Japanese native fowls infected with ALV.

Several reports have indicated the possibility that retroviruses have a direct role in the pathogenesis of myocarditis and dilated cardiomyopathy in humans, monkeys and other animals (Roldan *et al*., 1987; Gilka & Spencer, 1990; Gilka *et al*., 1991; Shannon *et al*., 2000; Iwata *et al*., 2002; Lewis *et al*., 2005; Brellou *et al*., 2007), although the relationship between retrovirus infection and cardiac abnormality remains obscure. Whether HIV-1 and SIV can infect cardiomyocytes is still controversial (Grody *et al*., 1990, Rebolledo *et al*., 1998), whereas the fact that ALV has strong tropism for cardiomyocytes and Purkinje fibres is evidenced by the frequent formation of matrix inclusion bodies in these cells (Gilka & Spencer, 1985; Nakamura *et al*., 1988; Nakamura *et al*., 2007). Despite these different degrees of tropism for cardiomyocytes, ALV-induced myocardial alteration is considered to be useful for clarifying the pathogenesis of retroviral cardiomyopathy.

In conclusion, these results indicate that several strains of ALVs could promote growth activity of cardiomyocytes and induce cardiomyocyte hypertrophy by a

mechanism other than promoter insertion. This is the first report showing unique hypertrophy and growth of cardiomyocytes induced by ALV. This animal model may provide new insight into retrovirus-induced cardiac pathology.

Summary

Unusual cardiomyocyte hypertrophy and mitosis were observed in Japanese native fowls infected with ALVs-A. The affected hearts were evaluated by histopathology and immunohistochemistry, viral isolation, viral genome sequencing and experimental infection. There was non-suppurative myocarditis in eighteen fowls and seven of them had abnormal cardiomyocytes, which were distributed predominantly in the left ventricular wall and showed hypertrophic cytoplasm and atypical large nuclei. Nuclear chains and mitosis were frequently noted in these cardiomyocytes and immunohistochemistry for PCNA supported the enhancement of mitotic activity. ALVs were isolated from all affected cases and phylogenic analysis of *env*SU genes showed that the isolates were mainly classified into two different clusters, suggesting genetic diversity. *In ovo* experimental infection with two of the isolates was demonstrated to cause myocarditis and cardiomyocyte hypertrophy similar to those in the naturally occurring lesions and cardiac hamartoma (rhabdomyoma) in a shorter period of time (at 35 days of age) than expected. These results indicate that ALVs cause myocarditis as well as cardiomyocyte abnormality in chickens, implying a pathogenic mechanism different from promoter insertion and the existence of retrovirus-induced heart disorder.

General conclusion

Fowl glioma is histologically characterized by multiple nodular astrocytic growths with disseminated non-suppurative encephalitis. The first case was reported in Spain in 1935. This disease has been described as various entities and the aetiology and pathogenesis had long been controversial. In 1995, the first case of fowl glioma in Japan was found in Japanese native fowls and subsequent experimental studies demonstrated that the disease is caused by fowl glioma-inducing virus (FGV) prototype, belonging to subgroup A of avian leukosis virus (ALV-A) and that this strain could also induce cerebellar hypoplasia and perineurioma in chickens. These results indicate that FGV prototype is a unique ALV that cause glioma and other neurological disorders. Additionally, epidemiological studies showed that FGVs, including FGV prototype and the variants, have been prevalent among ornamental chickens in Japan.

The long terminal repeat (LTR) and *env* gene are known to play important roles in the oncogenicity and tissue tropism of ALV. However, whether FGV variants with mutations and deletions of nucleotides of the *env* have neurotropism and/or gliomagenicity remains unclear. In the meanwhile, rare conditions, including cerebellar anomaly in specific-pathogen-free (SPF) White Leghorn chickens and unusual cardiac abnormality in Japanese native fowls, were recently found. These lesions were pathologically suspected to be due to the infection with FGVs or other strains. Thus, to further clarify pathogenesis of FGVs, experimental infection with the FGV variants, analysis of intracerebral cytokine expressions in the early infection phase, and pathological and molecular biological analyses on cerebellar anomaly in White Leghorn chickens and cardiac abnormality in Japanese native fowls were performed.

In Chapter I, the complete nucleotide sequences of four FGV variants, including Tym-43, U-1, Sp-40 and Sp-53, were determined and their pathogenicity was investigated to clarify whether or not these strains have the ability to induce brain lesions. The sequences of the surface (SU) proteins encoded by *env* of these viruses had 85 to 95% identity with the corresponding region of FGV prototype. Phylogenic analysis based on *env*SU showed that Tym-43, U-1 and FGV prototype grouped together in a cluster, but Sp-40 and Sp-53 formed a completely separate cluster. Next, SPF chickens were inoculated with these variants as well as the chimeric virus RCAS (A)-(FGV*env*SU), constructed by substituting the SU region of FGV prototype into the retroviral vector RCAS (A). The four variants induced glioma and cerebellar hypoplasia and the birds inoculated with Sp-53 had the most severe lesions. In contrast, RCAS (A)-(FGV*env*SU) provoked only mild non-suppurative inflammation. These results suggest that the ability to induce brain lesions similar to those of the FGV prototype is still preserved in these FGV variants and the *env*SU is not a crucial determinant to the glioma-inducibility of FGVs.

In Chapter II, the relationship between intracerebral replication of Sp-53, which has induced the most severe lesions in Chapter I, and astrocytic growth in the early infection phase was investigated. Replication abilities of two ALV strains, Sp-53 and RCAS (A), were compared in the brains of SPF chickens at 35 days of age. Sp-53 replicated faster than RCAS (A), and the histological score and the RNA level of IL-1β in brains were increased depending on the level of intracerebral viral RNA. Up-regulation of IL-1β was also demonstrated in primary cultured astrocytes. These results imply that the astrocytic growth in this phase is enhanced through the autocrine/paracrine production of IL-1β in the FGVs-infected astrocytes.

As described above, FGVs could induce cerebellar hypoplasia, which is rare condition in birds. In Chapter III, cerebellar anomalies from seven SPF White Leghorn chickens (*Gallus gallus domesticus*) were examined to clarify the morphological characteristics of affected cerebellums and the relationship between them and ALV infection. Grossly, the cerebellums showed disorganization of cerebellar folia and the macroscopic change was closely similar to that of FGV-induced cerebellar hypoplasia. Histologically, islands of heterotopic cortex were distributed from deeper cortices to the medulla in the cerebellum. The characteristic lesions were composed of randomly admixed components of cerebellar cortex, including soma of Purkinje cells, dendrites of Purkinje cells in the molecular layer and granular cells. Immunofluorescence analysis revealed Purkinje cells with haphazardly extended dendrites and a lack of Bergmann's glial fibres in the foci. Chicken parvovirus and ALVs were not detected in the affected birds by PCR. From these results, the lesions were diagnosed as cerebellar dysplasia and quite different from FGV-induced cerebellar lesions. This is the first description of cerebellar dysplasia in chickens possibly caused by a genetic abnormality.

Unusual cardiomyocyte hypertrophy with mitosis was recently observed in Japanese native fowls infected with ALVs. In Chapter IV, the affected hearts were evaluated by histopathology and immunohistochemistry, viral isolation, viral genome sequencing and experimental infection. There were non-suppurative myocarditis and abnormal cardiomyocytes characterized by hypertrophic cytoplasm and atypical large nuclei in the affected hearts. Nuclear chains, mitosis and matrix inclusions were frequently noted in these cardiomyocytes. ALVs were isolated from all affected birds and phylogenic analysis of *env*SU showed that isolates were mainly classified into two different clusters. *In ovo* experimental infection with two of the isolates was demonstrated to cause

myocarditis and cardiomyocyte hypertrophy similar to those in the naturally occurring lesions and cardiac hamartoma (rhabdomyoma) in a shorter period of time (at 70 days of age) than expected. These results indicate that ALVs cause cardiomyocyte abnormality in chickens, implying a pathogenetic mechanism different from promoter insertion and the existence of retrovirus-induced heart disorder.

The present studies suggest that FGV variants preserve ability to induce brain lesions similar to those of the FGV prototype and that production of IL-1β from astrocytes could mediate astrocytic growth in the early phase of the infection. In addition, these studies demonstrated that several strains of ALVs isolated from Japanese native fowls could promote growth activity of cardiomyocytes and induce cardiomyocyte hypertrophy. These results indicate that there is genetic and pathogenetic diversity among FGVs and the related ALVs, which still spread among Japanese native fowls in Japan.

References

Adams, S. C., Xing, Z., Li, J. & Cardona, C. J. (2009). Immune-related gene expression in response to H11N9 low pathogenic avian influenza virus infection in chicken and Peking duck peripheral blood mononuclear cells. Molecular immunology, 46, 1744-1749.

Akar, S. & Sur, E. (2010). The development of chicken cerebellar cortex and the determination of AgNOR activity of the Purkinje cell nuclei. Belgian Journal of Zoology, 140, 216-224.

Armién, A. G., McRuer, D. L., Ruder, M. G. & Wünschmann, A. (2013). Purkinje cell heterotopy with cerebellar hypoplasia in two free-living American kestrels (*Falco sparverius*). Veterinary Pathology, 50, 182-187.

Arshad, S. S., Smith, L. M., Howes, K., Russell, P. H., Venugopal, K. & Payne, L. N. (1999). Tropism of subgroup J avian leukosis virus as detected by in situ hybridization. Avian Pathology, 28, 163-169.

Ayyavoo, V., Mahalingam, S., Rafaeli, Y., Kudchodkar, S., Chang, D., Nagashunmugam, T., Williams, W. V. & Weiner, D. B. (1997). HIV-1 viral protein R (Vpr) regulates viral replication and cellular proliferation in T cells and monocytoid cells in vitro. Journal of Leukocyte Biology, 62, 93-99.

Bai, J., Payne, L. N. & Skinner, M. A. (1995). HPRS-103 (exogenous avian leukosis virus, subgroup J) has an *env* gene related to those of endogenous elements EAV-0 and E51 and an E element found previously only in sarcoma viruses. Journal of Virology, 69, 779-784.

Barbour, E. K., Bouljihad, M., Hamdar, B., Sakr, W., Eid, A. & Safieh-Garabedian, B. (1999). Dynamics of protein 27 of avian leukosis virus and transforming growth factor beta2 in lymphoid leukosis susceptible and resistant broiler chicken breeding stock. Veterinary Research Communications, 23, 191-200.

Beard, J. W. (1980). Biology of avian oncornaviruses. In G. Klein ed. Viral oncology (pp. 55-87). New York: Ravan Press.

Belmonte, V. (1935). Über ein Glioma beim Haushuhn. Virchows archive für Pathologische Anatomie and Physiologie und für Klinische Medizin, 294, 329-333.

Benyounes, N., Fohlen, M., Devys, J. M., Delalande, O., Moures, J. M. & Cohen, A. (2012). Cardiac rhabdomyomas in tuberous sclerosis patients: a case report and review of the literature. Archives of Cardiovascular Diseases, 105, 442-445.

Biering-Sørensen, U. (1956). On disseminated, focal gliomatosis (“multiple gliomas”) and cerebral calcification in hens. A study of pathogenesis. Nordisk Veterinaer Medicin, 8, 887-901.

Bieth, E. & Darlix, J. L. (1992). Complete nucleotide sequence of a highly infectious avian leukosis virus. Nucleic Acids Research, 20, 367.

Bowles, N. E., Eisenemith, R. C., Mohuiddin, R., Pyron, M. & Woo, S. L. C. (1996). A simple and efficient method for the concentration and purification of recombinant retrovirus for increased hepatocyte transduction *in vivo*. Human Gene Therapy, 7, 1735-1742.

Brellou, G. D., Angelopoulou, K., Poutahidis, T. & Vlemmas, I. (2007). Detection of maedi-visna virus in the liver and heart of naturally infected sheep. Journal of Comparative Pathology, 136, 27-35.

Brown, D. W. & Robinson, H. L. (1988). Influence of *env* and long terminal repeat sequences on the tissue tropism of avian leukosis viruses. Journal of Virology, 62, 4828-4831.

Cerri, S., Piccolini, V. M. & Bernocchi, G. (2010). Postnatal development of the central nervous system: anomalies in the formation of cerebellum fissures. The Anatomical Record, 293, 492-501.

Chang, K. S., Lee, S. I., Ohashi, K., Ibrahim, A. & Onuma, M. (2002). The detection of the *meq* gene in chicken infected with Marek's disease virus serotype 1. The Journal of Veterinary Medical Science, 64, 413-417.

Chesters, P. M., Howes, K., Petherbridge, L., Evans, S., Payne, L. N. & Venugopal, K. (2002). The viral envelope is a major determinant for the induction of lymphoid and myeloid tumors by avian leukosis virus subgroups A and J, respectively. Journal of General Virology, 83, 2553-2561.

Corrales, J. D., Blaess, S., Mahoney, E. M. & Joyner, A. L. (2006). The level of sonic hedgehog signaling regulates the complexity of cerebellar foliation. Development, 133, 1811-1821.

Coyle-Rink, J., Sweet, T. M., Abraham, S., Sawaya, B. E., Batuman, O., Khalili, K. & Amini, S. (2002). Interaction between TGF-β signaling proteins and C/EBP controls basal and Tat-mediated transcription of HIV-1 LTR in astrocytes. Virology, 299, 240-247.

Dang, Q., Whitted, S., Goeken, R. M., Brenchley, J. M., Matsuda, K., Brown, C. R., Lafont, B. A. P., Starost, M. F., Iyengar, R., Plishka, R. J., Buckler-White, A. & Hirsch, V. M. (2012). Development of neurological disease is associated with increased immune activation in simian immunodeficiency virus-infected macaques. Journal of Virology, 86, 13795-13799.

De Castro, S., d'Amati, G., Gallo, P., Cartoni, D., Santopadre, P., Vullo, V., Cirelli, A. & Migliau, G. (1994). Frequency of development of acute global left ventricular dysfunction in human immunodeficiency virus infection. Journal of the American College of Cardiology, 24, 1018-1024.

Dorn G. W. II. & Force, T. (2005). Protein kinase cascades in the regulation of cardiac hypertrophy. The Journal of Clinical Investigation, 115, 527-537.

Ellison, D., Love, S., Chimelli, L., Harding, B. N., Lowe, J. & Vinters, H. V. (2004). Malformations. In D. Ellison & S. Love. Neuropathology 2nd edn (pp. 95-99). Edinburgh: Mosby.

Ewert, D.L., Steiner, I. & DuHadaway, J. (1990). In ovo infection with the avian retrovirus RAV-1 leads to persistent infection of the central nervous system. Laboratory Investigation, 62, 156-162.

Fadly A.M. & Nair V. (2008). Leukosis/sarcoma group. In A.M. Fadly I. Davidson Diseases of Poultry, 12th edn (pp. 514-568). Ames, IA: Blackwell Publishing.

Gibson, M. S., Kaiser, P. & Fite, M. (2014). The chicken IL-1 family: evolution in the context of the studied vertebrate lineage. Immunogenetics, 66, 427-438.

Gilka, F. & Spencer, J. L. (1985). Viral matrix inclusion bodies in myocardium of lymphoid leukosis virus-infected chickens. American Journal of Veterinary Research, 46, 1953-1960.

Gilka, F. & Spencer, J. L. (1990). Chronic myocarditis and circulatory syndrome in a White Leghorn strain induced by an avian leukosis virus: light and electron microscopic study. Avian Diseases, 34,

174-184.

Gilka, F., Spencer, J. L. & Chambers, J. R. (1991). Response of meat-type chickens to infection with RAV-1 avian leukosis virus. Avian Pathology, 20, 637-647.

GrantMaxie, M. & Robinson, W. F. (2007). Cardiovascular system. In M. GrantMaxie (ed.) Jubb, Kennedy, and Palmer's Pathology of domestic animals. 5th edn. (pp. 1-103). Philadelphia, PA: Saunders Elsevier.

Grody, W. W., Cheng, L. & Lewis, W. (1990). Infection of the heart by the human immunodeficiency virus. The American Journal of Cardiology, 66, 203-206.

Guo, H., Gao, J., Taxman, D. J., Ting, J. P. Y. & Su, L. (2014). HIV-1 infection induces interleukin-1β production via TLR8 protein-depedent and NLRP3 inflammasome mechanisms in human monocytes. The Journal of Biological Chemistry, 289, 21716-21726.

Hafner, S., Williams, S. M. & Sutton, M. T. (2007). Retroviral inclusions in the enteric smooth muscle of a tumor-bearing young chicken. Avian Diseases, 51, 133-136.

Hatai, H., Ochiai, K., Murakami, M., Imanishi, S., Tomioka, Y., Toyoda, T., Ohashi, K. & Umemura, T. (2008a). Prevalence of fowl glioma-inducing virus in chickens of zoological gardens in Japan and nucleotide variation in the *env* gene. The Journal of Veterinary Medical Science, 70, 469-474.

Hatai, H., Ochiai, K., Nagakura, K., Imanishi, S., Ochi, A., Kozakura, R., Ono, M., Goryo, M.,Ohashi, K.& Umemura, T. (2008b). A recombinant avian leukosis virus associated with fowl glioma in layer chickens in Japan. Avian Pathology, 37, 127-137.

Hatai, H., Ochiai, K., Tomioka, Y., Toyoda, T., Hayashi, K., Anada, M., Kato, M., Toda, A.,Ohashi, K., Ono, E., Kimura, T. & Umemura, T. (2005). Nested polymerase chain reaction for detection of the avian leukosis virus causing so-called fowl glioma. Avian Pathology, 34, 473-479.

Heckroth, J. A., Goldowitz, D. & Eisenman, L. M. (1989). Purkinje cell reduction in the reeler mutant mouse: a quantitative immunohistochemical study. Journal of Comparative Neurology, 279, 546-555.

Heidrich, J. E., Adcock, M. A., Bolin, C., Cheville, N. F. & Smith, R. E. (1987). Effect of Rous associated virus number 7 on lymphoid cells and tissues of the chicken. Veterinary Immunology and Immunopathology, 15, 267-283.

Hill, J. J., Tremblay, T., Cantin, C., O'Conner-McCourt, M., Kelly, J. F. & Lenferink, A. E. G. (2009). Glycoproteomic analysis of two mouse mammary cell lines during transforming growth factor (TGF)-β induced epithelial to mesenchymal transition. Proteome Science, 7:2, doi:10.1186/1477-5956-7-2.

Hughes, S. H. (2004). The RCAS vector system. Folia Biologica, 50, 107-119.

Hughes, S.H., Greenhouse, J.J., Petropoulos, C.J. & Sutrave, P. (1987). Adaptor plasmids simplify the insertion of foreign DNA into helper-independent retroviral vectors. Journal of Virology, 61, 3004-3012.

Hull, S., Lim, J., Hamil, A., Nitta, T. & Fan, H. (2012). Analysis of jaagsiekte sheep retrovirus (JSRV) envelope protein domains in transformation. Virus Genes, 45, 508-517.

Iwata, N., Ochiai, K., Hayashi, K., Ohashi, K. & Umemura, T. (2002). Avian retrovirus infection

causes naturally occurring glioma; isolation and transmission of a virus from so-called fowl glioma. Avian Pathology, 31, 193-199.

Jackson, C. (1954). Glioma of the domestic fowl. Onderstepoort Journal of Veterinary Research, 26, 501-597.

Jacob, A. J., Sutherland, G. R., Bird, A. G., Brettle, R. P., Ludlam, C. A., McMillan, A. & Boon, N. A. (1992). Myocardial dysfunction in patients infected with HIV: prevalence and risk factors. British Heart Journal, 68, 549-553.

Jakowlew, S. B. (2006). Transforming growth factor-β in cancer and metastasis. Cancer and Metastasis Reviews, 25, 435-457.

Jensen, P., Zoghbi, H. Y. & Goldowitz, D. (2002). Dissection of the cellular and molecular events that position cerebellar Purkinje cells: a study of the *math 1* null-mutant mouse. The Journal of Neuroscience, 22, 8110-8116.

Jobling, S. A., Auron, P. E., Gurka, G., Webb, A. C., McDonald, B., Rosenwasser, L. J. & Gehrke, L. (1988). Biological activity and receptor binding of human prointerleukin-1β and subpeptides. The Journal of Biological Chemistry, 263, 16372-16378.

Johnson, A. L., Bridgham, J. T., Munks, M. & Witty, J. P. (1998). Characterization of the chicken interleukin-1β converting enzyme (caspase-1) cDNA and expression of caspase-1 mRNA in the hen. Gene, 219, 55-62.

Jungherr, E. & Wolf, A. (1939). Gliomas in animals: a report of two astrocytomas in the common fowl. The American Journal of Cancer, 37, 493-509.

Kaiser, P., Rothwell, L., Galyov, E. E., Barrow, P. A., Burnside, J. & Wigley, P. (2000). Differential cytokine expression in avian cells in response to invasion by *Salmonella typhimurium*, *Salmonella enteritis* and *Salmonella gallinarum*. Microbiology, 146, 3217-3226.

Kitano, Y., Yasuda, N., Shimizu, T., Ohzono, H. & Iwamoto, T. (1997). Teratogenicity of Aino virus in the chick embryo. Research in Veterinary Science, 62, 195-198.

Lewis, W., Miller, Y. K., Haase, C. P., Ludaway, T., McNaught, J., Russ, R., Steltzer, J., Folpe, A., Long, R. & Oshinski, J. (2005). HIV viral protein R causes atrial cardiomyocyte mitosis, mesenchymal tumor, dysrhythmia, and heart failure. Laboratory Investigation, 85, 182-192.

Luginbühl, H., Fankhauser, R. & McGrath, J.T. (1968). "Spontaneous neoplasms of the nervous system in animals". In Progress in Neurological Surgery, Edited by: Krayenbühl, H., Maspes, P.E. and Sweet, W.H. Vol. 2, 85-164. Chicago, IL: Year Book Medical Publishers.

Maeda, N., Fan, H. & Yoshikai, Y. (2008). Oncogenesis by retroviruses: old and new paradigms. Reviews in Medical Virology, 18, 387-405.

Marusak, R. A., Guy, J. S., Abdul-Aziz, T. A., West, M. A., Fletcher, O. J., Day, J. M., Zsak, L. & Barnes, H. J. (2010). Parvovirus-associated cerebellar hypoplasia and hydrocephalus in day old broiler chickens. Avian Diseases, 54, 156-160.

Massagué, J. (2008). TGF-β in cancer. Cell, 134, 215-230.

Matsuda, K., Brown, R. C., Foley, B., Goeken, R., Whitted, S., Dang, Q., Wu, F., Plishka, R., Buckler-White, A. & Hirsch, V. M. (2013). Laser capture microdissection assessment of virus

compartmentalization in the central nervous systems of macaques infected with neurovirulent simian immunodeficiency virus. Journal of Virology, 87, 8896-8908.

Maxie, M. G. & Youssef, S. (2007). Nervous system. In M. G. Maxie (Ed.). Jubb, Kennedy, and Palmer's Pathology of Domestic Animals 5th edn, vol.1 (pp. 309-314). Philadelphia, PA: Saunders Elsevier.

McGeady, T. A., Quinn, P. J. & FitzPatrick, E. S. (2006). Nervous system. In T. A. McGeady, P. J. Quinn & E. S. FitzPatrick (Eds.). Veterinary Embryology 1st edn (pp. 153-182). Oxford: Blackwell Publishing.

Merrill, J. E. & Chen, I. S. (1991). HIV-1, macrophages, glial cells, and cytokines in AIDS nervous system disease. The FASEB journal, 5, 2391-2397.

Miller, L. M., Van Vleet, J. F. & Gal, A. (2012). Cardiovascular and lymphatic vessels. In J. F. Zachary, M. D. McGavin (eds.). Pathologic basis of Veterinary diseases. 5th edn. (pp. 539-588). St. Louis: Elsevier Mosby.

Motitschke, A., Ottiger, H. P. & Jungbäck, C. (2010). Evaluation of the sensitivity of PCR methods for the detection of extraneous agents and comparison with in vivo testing. Biologicals, 38, 389-392.

Nakamura, K., Abe, F., Hihara, H. & Taniguchi, T. (1988). Myocardial cytoplasmic inclusions in chickens with hemangioma and lymphoid leukosis. Avian Pathology, 17, 3-10.

Nakamura, K., Higashi, T., Yamada, M., Imai, K. & Yamamoto, Y. (2007) Basophilic intracytoplasmic viral matrix inclusions distributed widely in layer hens affected with avian-leukosis-virus-associated tumours. Avian Pathology, 36, 53-58.

Ng, Y. P., Lee, S. M. Y., Cheung, T. K. W., Nicholls, J. M., Peiris, J. S. M. & Ip, N. Y. (2010). Avian influenza H5N1 virus induces cytopathy and proinflammatory cytokine responses in human astrocytic and neuronal cell lines. Neuroscience, 168, 613-623.

Nickel, R., Schummer, A. & Seiferle, E. (1973). Central nervous system. In R. Nickel, A. Schummer & E. Seiferle (Eds.). Anatomy of the Domestic Birds (pp. 114-130). Berli, Germany: Verlag Paul Parey.

Ochi, A., Ochiai, K., Kobara, A., Nakamura, S., Hatai, H., Handharyani, E., Tiemann, I., Tanaka 3rd, I. B., Toyoda, T., Abe, A., Seok, S., Sunden, Y., Torralba, N. C., Park, J., Hafez, H. M. & Umemura, T. (2012a). Epidemiological study of fowl glioma-inducing virus in chickens in Asia and Germany. Avian Pathology, 41, 299-309.

Ochi, A., Ochiai, K., Nakamura, S., Kobara, A., Sunden, Y. & Umemura, T. (2012b). Molecular characteristics and pathogenicity of an avian leukosis virus isolated from avian neurofibrosarcoma. Avian Diseases, 56, 35-43.

Ochiai, K., Ohashi, K., Mukai, T., Kimura, T., Umemura, T. & Itakura, C. (1999). Evidence of neoplastic nature and viral aetiology of so-called fowl glioma. Veterinary Record, 145, 79-81.

Ono, M., Tsukamoto, K., Tanimura, N., Haritani, M., Kimura, K.M., Suzuki, G., Okuda, Y. & Sato, S. (2004). An epizootic of subcutaneous tumors associated with subgroup A avian leukosis/sarcoma virus in young layer chickens. Avian Diseases, 48, 940-946.

Parvizi, P., Adbul-Careem, M. F., Haq, K., Thanthrige-Don, N., Schat, K. A. & Sharif, S. (2010). Immune responses against Marek's disease virus. Animal Health Research Reviews, 11, 123-134.

Patel, S. & Barkovich, A. J. (2002). Analysis and classification of cerebellar malformations. American Journal of Neuroradiology, 23, 1074-1087.

Peters, J. L., Cassone, V. M. & Zoran, M. J. (2005). Melatonin modulates intercellular communication among cultured chick astrocytes. Brain Research, 1031, 10-19.

Payne, L.N. (1998). HPRS-103: a retrovirus strikes back. The emergence of subgroup J avian leukosis virus. Avian Pathology, 27, S36-S45.

Rahimi, R. A. & Leof, E. B. (2007). TGF-β signaling: a tale of two responses. Journal of Cellular Biochemistry, 102, 593-608.

Rebolledo, M. A., Krogstad, P., Chen, F., Shannon, K. M. & Klitzner, T. S. (1998). Infection of human fetal cardiac myocytes by a human immunodeficiency virus-1-derived vector. Circulation Research, 83, 738-742.

Reece, R.L. (2008). Other tumors of unknown etiology. In Y.M. Saif , S. Hafner , A.M. Fadly ,J.R. Glisson , L.R. McDougald , L.K. Nolan & D.E. Swayne . Diseases of Poultry 12th edn (pp. 593-616). Ames, IA: Blackwell Publishing.

Rice, D. S. & Curran, T. (1999). Mutant mice with scrambled brains: understanding the signaling pathways that control cell positioning in the CNS. Genes & Development, 13, 2758-2773.

Roldan E. O., Moskowitz, L. & Hensley, G. T. (1987). Pathology of the heat in acquired immunodeficiency syndrome. Archives of Pathology & Laboratory Medicine, 111, 943-946.

Saule, S., Mérigaud, J. P., Al-Moustafa, A. E., Ferré, F., Rong, P. M., Amouyel, P., Quatannens, B., Stéhelin, D. & Dieterlen-Lièvre, F. (1987). Heart tumors specifically induced in young avian embryos by the v-*myc* oncogene. Proceedings of the National Academy of Sciences, 84, 7982-7986.

Schoen, F. J. & Mitchell, R. N. (2004). The heart. In V. Kumar, A. K. Abbas, N. Fausto & J. C. Aster. (Eds.). Robbins and Cotran Pathologic Basis of disease. 8th edn (pp.529-587). Philadelphia, PA: Saunders Elsevier.

Sen, E. (2011). Targeting inflammation-induced transcription factor activation: an open frontier for glioma therapy Drug Discovery Today, 16, 1044 -1051.

Shannon R. P., Simon, M. A., Mathier, M. A., Geng, Y. J., Mankad, S. & Lackner, A. A. (2000). Dilated cardiomyopathy associated with simian AIDS in nonhuman primates. Circulation, 101, 185-193.

Sharma, V., Dixit, D., Koul, N., Mehta, V. S. & Sen, E. (2011). Ras regulates interleukin-1β-induced HIF-1α transcriptional activity in glioblastoma. Journal of Molecular Medicine, 89, 123-136.

Shini, S., Shini, A. & Kaiser, P. (2010). Cytokine and chemokine gene expression profiles in heterophils from chickens treated with corticosterone. Stress, 13, 185-194.

Shivaprasad, H.L., Franca, M., Woolcock, P.R., Nordhausen, R., Day, J.M. & Pantin-Jackwood, M. (2009). Myocarditis associated with reovirus in turkey poults. Avian Diseases, 53, 523-532.

Stedman, N. L. & Brown, T. P. (2002). Cardiomyopathy in broiler chickens congenitally infected with avian leukosis virus subgroup J. Veterinary Pathology, 39, 161-164.

Sudarov, A. & Joyner, A. L. (2007). Cerebellum morphogenesis: the foliation pattern is orchestrated

by multi-cellular anchoring centers. Neural Development, 2, 26.

Summers, B.A., Cummings, J.F. & de Lahunta, A. (1995). Tumors of the central nervous system. In Veterinary Neuropathology (pp. 351 – 401). St Louis, MO: Mosby-Year Book.

Swayne, D.E., Fletcher, O.J., Abdul-Aziz, T., Shivaprasad, H.L. & Barnes, H.J. (2008). "Nervous system". In Fletcher, O.J. and Abdul-Aziz (Eds), Avian Histopathology, 3rd edn (pp. 260-291). Jacksonville, FL: American Association of Avian Pathologists.

Tanimoto, T. & Ohtsuki, Y. (1995). The pathogenesis of so-called cardiac rhabdomyoma in swine: a histological, immunohistochemical and ultrastructural study. Virchows Archiv, 427, 213-221.

Tarasiuk, K., Woźniakowski, G. & Samorek-Salamonowicz, E. (2012). Occurrence of chicken parvovirus infection in Poland. The Open Virology Journal, 6, 7-11.

Ten Dijke, P. & Hill, C. S. (2004). New insights into TGF-β-Smad signaling. Trends in Biochemical Sciences, 29, 265-273.

Thompson, J.D., Higgins, D.G. & Gibson, T.J. (1994). CLUSTAL W: improving the sensitivity of progressive multiple sequence alignment through sequence weighting, position-specific gap penalties and weight matrix choice. Nucleic Acids Research, 22, 4673-4680.

Tiwari, R., Bargman, W. & Bose Jr., H. R. (2011). Activation of the TGF-β/Smad signaling pathway in oncogenic transformation by v-Rel. Virology, 413, 60-71.

Tomioka, Y., Ochiai, K., Ohashi, K., Kimura, T. & Umemura, T. (2003). *In ovo* infection with an avian leukosis virus causing fowl glioma: viral distribution and pathogenesis. Avian Pathology, 32, 617-624.

Tomioka, Y., Ochiai, K., Ohashi, K., Ono, E., Toyoda, T., Kimura, T. & Umemura, T. (2004). Genome sequence analysis of the avian retrovirus causing so-called fowl glioma and the promoter activity of the long terminal repeat. Journal of General Virology, 85, 647-652.

Toyoda, T., Ochiai, K., Hatai, H., Murakami, M., Ono, E., Kimura, T. & Umemura, T. (2006). Cerebellar hypoplasia associated with an avian leukosis virus inducing fowl glioma. Veterinary Pathology, 43, 294-301.

Toyoda, T., Ochiai, K., Ohashi, K., Tomioka, Y., Kimura, T & Umemura, T. (2005). Multiple perineuriomas in chicken (*Gallus gallus domesticus*). Veterinary Pathology, 42, 176-183.

Tsukamoto, K., Hihara, H. & Kono, Y. (1991). Detection of avian leukosis virus antigens by the ELISA and its use for detecting infectious virus after cultivation of samples and partial characterization of specific pathogen-free chicken lines maintained in this laboratory. The Journal of Veterinary Medical Science, 53, 399-408.

Wang, G., Zhang, J., Li, W., Xin, G., Su, Y., Gao, Y., Zhang, H., Lin, G., Jiao, X. & Li, K. (2008). Apoptosis and proinflammatory cytokine responses of primary mouse microglia and astrocytes induced by human H1N1 and avian H5N1 influenza viruses. Cellular & Molecular Immunology, 5, 113-120.

Wang, V. Y. & Zoghbi, H. Y. (2001). Genetic regulation of cerebellar development. Nature Reviews Neuroscience, 2, 484-491.

Weiss, R.A. (1993). "Cellular receptors and viral glycoproteins involved in retrovirus entry". In Levy,

J.A (Eds). The Retroviruses (pp.1-108). New York: Plenum Press.

Wight, P.A.L. & Duff, R.H. (1964). The histopathology of epizootic gliosis and astrocytomata of the domestic fowl. Journal of Comparative Pathology and Therapeutics, 74, 373-380.

Xing, Q. H., Hayakawa, H., Izumo, K., Kubota, R., Gelpi, E., Budka, H. & Izumo, S. (2009). In vivo expression of proinflammatory cytokines in HIV encephalitis: an analysis of 11 autopsy cases. Neuropathology, 29, 433-442.

Yamanaka, R., Tanaka, R., Saitoh, T. & Okoshi, S. (1994). Cytokine gene expression on glioma cell lines and specimens. Journal of Neuro-oncology, 21, 243-247.

Yeung, Y. T., McDonald, K. L., Grewal, T. & Munoz, L. (2013). Interleukins in glioblastoma pathophysiology: implications for therapy. British Journal of Pharmacology, 168, 591-606.

Zavala, G., Pretto, C., Chow, Y. H. J., Jones, L., Alberti, A., Grego, E., De las Heras, M. & Palmarini, M. (2003). Relevance of Akt phosphorylation in cell transformation induced by Jaagsiekte sheep retrovirus. Virology, 312, 95-105.

Zink, M. C., Suryanarayana, K., Mankowski, J. L., Shen, A., Piatak, M. Jr., Spelman, J. P., Carter, D. L., Adams, R. J., Lifson, J. D. & Clements, J. E. (1999). High viral load in the cerebrospinal fluid and brain correlates with severity of simian immunodeficiency virus encephalitis. Journal of Virology, 73, 10480-10488.

Zsak, L., Strother, K. O. & Kisary, J. (2008). Partial genome sequence analysis of parvoviruses associated with enteric disease in poultry. Avian Pathology, 37, 435-441.

Summary in Japanese

(和文要旨)

鶏の神経膠腫 (fowl glioma) は非化膿性髄膜脳炎を背景に星状膠細胞が多発性結節性に増殖する鶏の疾患である。この疾患は 1935 年にスペインで初発例が報告されて以来，様々な疾患名で報告されてきたが，その原因や病態に関する詳細は不明のままであった。こうした中，国内では 1995 年に本疾患に罹患した日本鶏 (*Gallus gallus domesticus*) が初めて発見された。さらにその後の実験的研究によって，罹患脳から鶏白血病ウイルス A 亜群 (avian leukosis virus subgroup A; ALV-A) に属す鶏の神経膠腫誘発ウイルス (fowl glioma-inducing virus prototype; FGV prototype) が分離され，本ウイルスが本疾患の原因であること，ならびに本ウイルスは神経膠腫のほか，小脳低形成ならびに神経周膜腫を誘発することが証明された。これら成績は FGV prototype が神経膠腫やほかの神経系疾患を引き起こすユニークな ALV であることを示している。また，疫学的研究により FGV prototype と FGV 変異株を含む FGVs は国内の日本鶏に蔓延していることが明らかにされている。

ALV の腫瘍原性と組織親和性を規定する因子として long terminal repeat (LTR) と *env* 遺伝子が重要な役割を果たしており，誘発腫瘍の種類を規定する主な因子は *env* であることが示唆されている。しかし，*env* に塩基の置換や欠損を持つ FGV 変異株が神経親和性と神経膠腫誘発能の両者, あるいはいずれか一方を保持しているかは未だ不明である。一方，最近になって Specific-Pathogen-Free (SPF) 白色レグホン種の小脳異常や日本鶏の心筋異常といった, FGVs や 他の ALV 株との関連が疑われるまれな病態が新たに見出され

た。以上の背景を踏まえ，本研究では FGVs の病原性やその規定因子をより明確にするため，FGV 変異株の病原性ならびに感染初期の脳内サイトカインと脳病変との関連を解析した。また， 白色レグホンの小脳異常および日本鶏の心筋異常の病理学的ならびに分子生物学的解析を実施した。

第 I 章では FGV 変異株 4 株 (Tym-43, U-1, Sp-40 および Sp-53) の脳病変誘発能を調べるため，これら変異株のウイルスゲノム全長のシークエンス解析を行い，さらに実験感染鶏の脳病変を比較した。シークエンス解析では変異株の *env*SU は FGV prototype のそれと 85～95%の相同性を示し，同領域の分子系統樹では Tym-43，U-1 および FGV prototype は同じクラスターに分類されたが，Sp-40 と Sp-53 は別のクラスターに分類された。次にこれら 4 株とトリレトロウイルスベクター RCAS (A) に FGV prototype の *env*SU を組み込んだキメラウイルスを用いて感染実験を行った。組織学的には いずれの変異株も小脳低形成と神経膠腫を誘発し， Sp-53 が最も顕著な病変を誘発した。一方，キメラウイルス接種鶏では脳に軽度の囲管性リンパ球浸潤が認められたのみであった。以上の成績から，FGV 変異株には FGV prototype と同様の神経病原性が保持されていること，ならびに *env*SU は神経膠腫誘発能の決定因子ではないことが明らかになった。

第 II 章では，第 I 章において最も強い病変を誘発した Sp-53 を用いて感染実験を行い，感染初期の脳内ウイルス量と星状膠細胞の増殖との関連性を解析した。まず初めに Sp-53 と RCAS (A) の脳内ウイルス増殖量を 35 日齢時の鶏で比較した。その結果，Sp-53 は RCAS (A) よりも早く増殖し，Sp-53 の脳内ウイルス RNA 量が増加するにつれて脳病変スコアと脳内の IL-1β mRNA 発現量が増加することが判明した。また， IL-1β の発現量増加は Sp-53 を感染させた初代鶏星状膠細胞内でも確認された。以上の成績から，感染初期にみられる星状膠細胞

の増殖は星状膠細胞内でのウイルス複製とこれに続く IL-1β の産生がオートクライン・パラクライン的に作用して促進される可能性が示唆された。

上述の通り, FGVs は鳥類ではまれな小脳低形成を誘発する。第 III 章では SPF 白色レグホン種の鶏 (*Gallus gallus domesticus*) 7 羽に発生した小脳異常の病理学的特徴および ALV 感染との関連を明らかにするため, 罹患鶏の小脳を病理学的および分子生物学的に解析した。肉眼的に罹患小脳は小脳回の無秩序な配列を示し，FGVs による小脳低形成ときわめて類似していた。組織学的には異所性小脳皮質が小脳虫部の皮質深部から髄質にかけて島状に分布し，これら特徴的な病巣はプルキンエ細胞の細胞体と樹状突起，および顆粒細胞を含む皮質成分の無秩序な混在からなっていた。免疫蛍光染色標本では異所性皮質内に放射状に伸びた樹状突起を持つプルキンエ細胞が確認されたが， GFAP 陽性となる Bergmann グリア線維は観察されなかった。また, 鶏パルボウイルスおよび ALVs は PCR により検出されなかった。以上の成績から，本病変は小脳異形成と考えられ，FGVs 感染に起因する小脳病変とは大きく異なることが明らかとなった。本成績は遺伝性が原因として疑われる鶏の小脳異形成に関する初めての記載である。

近年, ALVs 感染日本鶏の心臓に通常認められない心筋細胞の肥大と有糸分裂像が認められた。第 IV 章では，これら心筋病変を病理学的および免疫組織学的に解析するとともに，分離した ALV 株のシークエンス解析と感染実験を行った。組織学的には検索した心臓には筋形質内基質封入体を伴う非化膿性心筋炎と筋形質の肥大と巨大な異型核を有する異常心筋細胞が認められた。また，これら心筋細胞には核鎖，有糸分裂像と基質封入体が頻繁に認められた。検索した野外例すべてから ALVs が分離され，*env*SU に基づく分子系統樹では分離株は 2 つの異なるクラスターに分類された。分離株のうち 2 株を卵黄嚢内接種し

た感染実験により，これら ALVs は 70 日という短い期間で野外例と同様の心筋炎と心筋細胞の肥大，さらに心臓過誤腫（心臓横紋筋腫）を誘発することが証明された。以上の成績から，ALVs は心筋の形態異常を誘発することが明らかとなった。本成績はこれら心筋異常の発生にはプロモーター挿入以外の発生機序が関与すること，また，レトロウイルス感染症は心疾患の原因となりうることを示していると思われる。

以上の成績をまとめると，本研究によって FGV 変異株には FGV prototype と同様の神経病原性が保持されていること，ならびに感染初期の星状膠細胞の増殖は感染細胞に由来する IL-1β に関連して生じることが示唆された。さらに，本研究によって日本鶏由来 ALVs の中には心筋細胞の増殖活性を促進し，細胞の肥大を引き起こすウイルスが存在することが明らかになった。これら成績はわが国の日本鶏に蔓延している FGVs や これらと近縁な ALVs 間には遺伝子および病原性の多様性がみられることを示している。

Dedicated to my family and friends...